TABLE 2

Titer of HIV-1-puro Packaged in Murine 3T3 Cells Pseudotyped with VSV-G after Heterokaryon Formation between Human or Mink Cells

	No. of Puro^r colonies on HOShCD4hCCR5[a]	
Fusion partner	0.5 ng[b]	5 ng
HeLa	16 ± 3[c]	43 ± 15
Mv.1.Lu	20 ± 6	52 ± 12
NIH 3T3	2 ± 1	7 ± 2

[a] HOS cells expressing both CD4 and CCR5.
[b] Input virus.
[c] Results are means ± standard deviations for duplicate determinations.

assembly-resistant phenotype seen in murine NIH 3T3 cells can be complemented by phenotypic mixing with human as well as mink cells.

To verify that heterokaryons from murine and human or mink cells were also able to support the production of infectious virus, murine NIH 3T3-hCycT1 expressing HIV-1 *gag–pol* genes were transiently transfected with VSV-G vector and subsequently fused by PEG treatment with HeLa or Mv.1.Lu cells. The potential for pseudotyped viruses generated to infect hCD4hCCR5HOS cells was then determined. A greater than sevenfold increase in infectivity was observed for pseudotyped viruses produced from NIH 3T3 murine cells after heterokaryon formation between human or mink cells (Table 2). These findings clearly show that virions produced among murine cells can be rendered more infectious by phenotypic mixing with human as well as mink cells. This complementation in infectivity was a constant phenomenon in a large series of experiments. We conclude that murine NIH 3T3 cells lack some factor(s) necessary for the HIV-1 Gag assembly. These cellular cofactors appear to play crucial roles in mediating HIV-1 infectivity and are functional in both mink and human cells.

DISCUSSION

We obtained evidence for the heterogeneity in the potential of cells from small animal to support the late phase of HIV-1 replication. Among cells from nonhuman vertebrates, avian chicken embryonic fibroblasts (CEF), quail QT6, and mink (*Mustera vison*) lung Mv.1.Lu cells were found to support Gag assembly and release more efficiently than seen in rodent cells. A significant intraspecies variation was observed among rodent cells. Consistent with previous reports (Mariani *et al.*, 2000; Bieniasz and Cullen, 2001), the defects appear to be most profound in murine cells and can be partially overcome by fusion with permissive human cells (Tables 1 and 2), findings which suggest the requirement of a species-specific cellular factor(s) critical for HIV-1 assembly (Bieniasz and Cullen, 2001; Mariani *et al.*, 2001). However, this assembly cofactor does not appear to be human cell specific since HIV-1 Gag assembles efficiently in avian and mink cells (Fig. 1B), and fusion with mink cells also overcomes the assembly-defective phenotype seen in murine cells (Fig. 5). Indeed, efficient HIV-1 particle assembly and release has been reported to occur even in insect cells (Gheysen *et al.*, 1989).

The basis for the defect in infectious virus production in murine cells appears to be multiple. Gag gene expression was reduced in rodent cells, even in the presence of hu-cyclin T1 expression. Since Rev has been shown to be functional in rodent cells (Malim *et al.*, 1991), the lower expression of Gag expression could be due to instability of the unspliced transcripts that serve as mRNAs for the translation of Gag and Gag–Pol polyproteins. Alternatively, there is inefficient transcription even in the presence of heterologous hu-cyclin T1.

In addition to reduced Gag gene expression, defects in Gag trafficking were also observed in murine cells. The myristoylation and basic motif in the N-terminal region of $Pr55^{gag}$ are predicted to contribute to membrane interactions via hydrophobic and electrostatic interactions, respectively. Gag defective in myristoylation was shown to form large cytosolic complexes (Hermida-Matsumoto and Resh, 2000). In addition, acquisition of a myristoylated and/or palmitoylated sequence from murine leukemia virus matrix or human Src family kinase Fyn protein was reported to increase the assembly of HIV-1 Gag in murine and human cells (Chen *et al.*, 2001; Lindwasser and Resh, 2001; Reed *et al.*, 2002). Data from our radiolabeling studies, however, show that $Pr55^{gag}$ synthesized in human and murine cells is myristylated to a comparable degree, indicating that the murine form of NMT is functional with regard to transfer of myristate from myristoyl-CoA to $Pr55^{gag}$. Nevertheless, this myristoylated $Pr55^{gag}$ in murine cells does not appear to traffic appropriately. Membrane floatation analyses indicate that HIV-1 Gag is not efficiently targeted to cell membranes in rodent species. Confocal microscopy reveals that whereas Gag is membrane associated in human cells, a diffused cytoplasmic presence is detected in murine cells.

Localization of Gag polyprotein predominantly in a cholesterol-rich region of the plasma membrane, known as lipid rafts, has recently been reported, and a model for assembly of both the HIV-1 Gag and Env in this membrane microdomain is emerging (Nguyen and Hildreth, 2000; Rousso *et al.*, 2000; Lindwasser and Resh, 2001; Ono and Freed, 2001). Since removal of Gag multimerization domains has shown to increase, rather than decrease, recovery of Gag proteins from lipid rafts (Lindwasser and Resh, 2001), the assembly defect is unlikely to be due to the inability of the myristoylated HIV-1 Gag polyproteins to multimerize in murine cells. Thus, it is

tempting to speculate that the basis for the defect in assembly and release of infectious HIV virions of rodent cells is inefficient targeting of Gag polyproteins to the plasma membrane. The function of a cellular cofactor(s) that facilitates HIV assembly therefore could be to target viral proteins specifically to the plasma membrane.

Gag polyprotein was also found to localize in the *trans* cisternae of the Golgi regions (Fig. 3). This result appears to be at odds with data showing that only Gag with mutations in the N-terminal basic residue cluster localizes to a region partly overlapping the *trans* medial region of the Golgi apparatus (Lindwasser *et al.*, 2001). The reason for this discrepancy is not clear but may be related to the use of different probes to monitor this organelle. When anticaveolin-1 MAb and rhodamine-labeled secondary antibody were used, overlay with EYFP-Mem, but not with EYFP-Golgi, was observed (data not shown). Caveolins are present in caveolae, flask-shaped invaginations of the plasma membrane where there is a subset of lipid rafts (Schnitzer *et al.*, 1995). These results may mean that HIV-1 Gag in human cells localized partly at or near the Golgi and TGN-proximal region as well as in plasma membrane.

The mink Mv.1.Lu cell line appears to support the postintegration steps of HIV-1 replication with few, if any, deficiencies compared to findings in human cell lines. The block of HIV-1 infection in mink cells has been shown to occur prior to proviral integration. Transfection of full-length HIV-1 DNA into mink cells results in productive infection (Levy *et al.*, 1986), and HIV-1 replication in mink cells has also been demonstrated using phenotypic mixing with amphotropic murine leukemia virus (Canivet *et al.*, 1990) or polyethylene glycol treatment following HIV-1 adsorption (Clapham *et al.*, 1991). Our data complement and extend these earlier studies of HIV-1 infection in this cell species. Species-specific blocks in the function HIV-1 Tat and Rev function are absent in mink cells. In fact, gene expression was comparable to that found in human cells in the absence of exogenous hu-cyclin T1 expression. HIV-1 Gag polyproteins synthesized traffick to the plasma membrane as efficiently as in human cells. Furthermore, HIV-1 replication in Mv.1.Lu cells expressing huCD4 and huCCR5 *in vitro* approaches the level seen in human hCD4hCCR5HOS cells (Koito *et al.*, unpublished data); thus the mink serves as a useful small animal model for HIV-1 infection and disease.

In conclusion, there is an assembly block in rodent cells, especially in murine cells. Among various vertebral species, cell lines derived from avian and mink support assemble and release of HIV-1 virions. These results imply that a key assembly cofactor(s) is functional not only in human cells but also in many other vertebrae, but is absent in some rodent species. Additional studies are required to characterize this block(s) through identification of a species-specific cellular factor(s) that interacts with HIV-1 Gag during viral assembly for the development of murine models. Identification of such a human factor(s) may lead to elucidation of new targets for therapeutic intervention in HIV-1 infection and disease.

MATERIALS AND METHODS

Plasmids and reagents

The hu-cyclin T1 gene was amplified from pRC12/CMV/huCycT1 (Bieniasz *et al.*, 1998; provided by B. R. Cullen, Duke University, Durham, NC) and inserted into pBluescript (SKII$^+$) and the retroviral vector pLXSN (Miller and Rosman, 1989, purchased from Clonetech, Palo Alto, CA) to yield pSKII/hCycT1 and pLXSN/hCycT1, respectively. In this recombinant retroviral vector, the viral genomic mRNA is produced by LTR derived from murine Moloney leukemia virus (MoMuLV) and the bacterial gene encoding resistance to G418 is initiated at an internal SV40 promoter. Vesicular stomatatis virus G (VSV-G)-expressing plasmids (pVSV-G) were obtained from Clonetech. SV40-based HIV-1 Env expressing vector pSM-SF162-*env* has been described elsewhere (Koito *et al.*, 1994). pHIV-puro, which encodes full-length HIV-1_{NL43} proviral DNA with a frameshift in the *env* gene, and the SV40 promoter regulating puromycin-resistant gene, was provided by R. Sutton (Stanford University Medical Center, Stanford, CA). Plasmid pEYFP vectors encode yellow-green fluorescent variants with four amino acid substitutions of the *A. victoria* GFP that is optimized for brighter fluorescence and higher expression in mammalian cells (Ormo *et al.*, 1996). pEYFP vectors fused with the N-terminal plasma membrane targetting signal of neuromodulin (pEYFP-Mem), the N-terminal 81 amino acids of the precursor to the human β-1,4-galactosyltransferase (pEYFP-Golgi) or endoplasmic reticulum (ER) targeting sequence of calreticulin, and the ER retention sequence, KDEL (pEYFP-ER) were from Clontech. All plasmids were purified from transformed *Escherichia coli* strain DH5α using the CONCERT High Purity Plasmid Maxiprep System (GIBCO BRL, Grand Island, NY).

Anti-p24CA (clone VAK4; IgG_{2b}) monoclonal antibody (MAb) was as described elsewhere (Koito *et al.*, 1988). Anti-p17MA (LG20-13-15) MAb was obtained from the Chemo-Sero-Therapeutic Research Institute (Kikuchi, Kumamoto, Japan). Anticaveolin-1 polyclonal antibody was from Santa Cruz Biotechnology (Santa Cruz, CA). Antimouse fluorescein isothiocyanate (FITC), antimouse rhodamine, and antirabbit rhodamine secondary antibodies were purchased from DAKO (Glostrup, Denmark).

Cells

The human T lymphoid cell line PM1, murine T lymphoma cell line EL4, BW5147, macrophage line RAW264, and WKA rat-derived myelomonocytic precursor cell line WRT7 (provided by M. Hosokawa; Hokkaido University,

Sapporo, Japan) were propagated in RPMI 1640 medium (GIBCO BRL). Human HeLa, 293T, the MoMuLV retroviral packaging cell line GP293 (CLONTECH), quail QT6, mink (*M. vision*) lung Mv.1.Lu (ATCC CCL-64), mouse muscle cell NOR10 (ATCC CCL-198), and fibroblast cell NIH3T3 were maintained in Dulbecco's modified Eagle's medium (GIBCO BRL). Chinese hamster ovary (CHO) K1 (ATCC CCL-61) cells were cultured in F-12 medium (Life Technologies, Rockville, MD). Chicken embryo fibroblasts (CEFs) were prepared and cultured as described (Shigekane *et al.*, 1999; provided by M. Sakaguchi; Kikuchi Research Center, Chemo-Sero-Therapeutic Research Institute). Human HOS cells stably expressing both the hu-CD4 molecule containing a cytoplasmic tail deletion and hu-CCR5 have been reported (Tahara-Hanaoka *et al.*, 2000). All media were supplemented with 10% heat-inactivated (56°C for 30 min) fetal bovine serum (GIBCO BRL) and cells were cultured at 37°C and 5% CO_2 in a humidified chamber.

Nonhuman animal cell lines expressing hu-cyclin T1 were generated by transducing cells with hu-cyclin T1 retroviral expression vector pLXRN/hCycT pseudotyped with VSV-G followed by 4 weeks of selection in the presence of 0.5 mg/ml of G418 (Geneticin; GIBCO BRL). This hu-cyclin-T1-expressing retrovirus was generated by cotransfecting GP293 cells with pLXSN/hCycT and pVSV-G. Replication-incompetent HIV-puro pseudotypes were generated by cotransfecting 293T cells with pHIV-puro and pVSV-G. Transfections were done using Lipofectamine 2000 (Life Technologies, Gaithersburg, MD) according to the manufacturer's instructions. Culture supernatants were harvested at 2 days posttransfection and stored at −70°C.

FACS analysis

Staining for intracytoplasmic HIV-1 p24 was done using the Fix and Perm reagents (Caltag Laboratories, Burlingame, CA), as described (Atchison *et al.*, 1996), using a MAb to p24 CA (VAK4) and FITC-conjugated goat antimouse IgG. The cells were then washed with Ca^{2+}-, Mg^{2+}-free phosphate-buffered saline PBS(−) and resuspended in staining medium (PBS(−), 0.05% NaN_3, and 3% FCS) containing propidium iodide (PI) (1 μg/ml). Amounts of intracellular p24 CA were then measured using a FACSCalibur (Beckton–Dickinson, San Jose, CA) by analyzing fluorescence using the Cell Quest software (Beckton–Dickinson).

Cell fractionation and sucrose floatation assays

The flotation assay was done as described (Spearman *et al.*, 1997) but with minor modifications. Cells (2×10^7) were harvested, rinsed twice with ice-cold PBS(−), resuspended in 300 μl of ice-cold hypotonic TE (10 mM Tris–HCl, pH 7.5, and 1 mM EDTA) buffer containing 10% (wt/vol) sucrose and a protease inhibitor cocktail (Roche; Mannheim, Germany) and then allowed to swell on ice for 15 min. These cells, then disrupted on ice by sonication (15 s, twice); nuclei and cell debris were pelleted by centrifugation (1000 *g* for 10 min at 4°C) and the resulting postnuclear extracts (250 μl) were then mixed with 1.25 ml of 85.5% (wt/vol) sucrose in TE buffer, adjusted to 80% (wt/vol) sucrose, placed at the bottom of a SW41 centrifuge tube, and overlaid with 65% (wt/vol) and 10% (wt/vol) sucrose in TE buffer. Standard volumes for this step gradient included 1.5 ml of 80% and 6 ml of 65% sucrose and the remaining portion of the centrifugation tube was filled with 10% sucrose in TE buffer. For centrifugation, we used a Beckman SW41 TI rotor at 30,000 rpm for 18 h at 4°C. Ten 1.0-ml fractions were collected from the top of the gradient. Aliquots of each fraction were separated by 15% polyacrylamide gel electrophophoresis containing sodium dodecyl sulfate (SDS–PAGE; Bio-Rad, Hercules, CA), transferred to polyvinylidine difluoride (PVDF) filters (Bio-Rad), and probed with a mixture of antibodies to p24 CA VAK4 and p17 MA LG20-13-15 followed by horseradish peroxidase-coupled protein G (Bio-Rad). Filters were developed using enhanced chemiluminescence reagents (ECL; Amersham, Buckinghamshire, England).

Immunofluorescence microscopy and confocal analysis

Cells transiently transfected with pEYFP-Mem, pEYFP-Golgi, or pEYFP-ER using Lipofectamine 2000 were reseeded into 35-mm poly-L-lysine-coated dish coverslips (Matsunami Glass Co., Osaka, Japan) and grown for 24 h at 37°C in DMEM containing 10% FCS, then fixed with 3.7% formaldehyde in PBS(−) for 15 min, permeabilized with 0.05% saponin and 0.2% bovine serum albumin (BSA) in PBS for 10 min at room temperature, and subsequently washed twice in PBS. For antibody staining, coverslips were incubated in a humid chamber at 37°C for 1 h with a MAb to p24 CA VAK4 for 1 h and with a rhodamine-conjugated rabbit antimouse IgG for 30 min at the appropriate dilution in 1% BSA and 0.02% Na azide in PBS(−). After three washings with PBS(−), these cells were mounted with FLUORESCENT MOUNTING MEDIUM (DAKO). For confocal microscopy, images were acquired with a Plan-Neofluar 100× oil immersion objective (Zeiss, Tokyo, Japan) and a Zeiss LSM 510 inverted laser scanning microscope. Beams (488 nm for FITC, 543 nm for He–Ne) from an argon and He–Ne laser were used. For two-color analysis, green and red emissions were simultaneously recorded through appropriate filters (505- to 530-nm bandpass filter for FITC and 585-nm long-pass filter for rhodamine) and stored in separate (red and green) image channels. Image quality was enhanced during data acquisition using the LSM line average feature. Postacquisition digital image enhancement was done using the LSM software.

N-Myristoylation

[9,10(n)-^{3}H]Myristic acid (catalog No. TRK907; Amersham), which was supplied in ethanol, was first vacuum dried and dissolved in dimethyl sulfoxide. Cells were metabolically labeled overnight with [9,10(n)-^{3}H]myristic acid (0.5 mCi/ml) in DMEM medium supplemented with 10% FCS. The cells were washed twice with PBS(−) and lysed in the radioimmunoprecipitation (RIPA; 0.15 M NaCl, 0.05 M Tris–HCl, pH 7.2, 1% Triton X-100, 1% sodium deoxycholate, and 0.1% sodium dodecyl sulfate) buffer containing a protease inhibitor cocktail (Roche). Proteins were immunoprecipitated with anti-p24 CA MAb VAK4 followed by immobilization on protein G–Sepharose (Amersham Pharmacia Biotech AB, Uppsala, Sweden). The immunoprecipitate was washed three times with RIPA buffer and solubilized in Laemmli's sample buffer. The radiolabeled proteins were size-fractionated by 10% SDS–PAGE, followed by autoradiography.

Pseudotyped virus production and transduction

HeLa, mink Mv.1.Lu, or murine NIH 3T3 carrying hucyclin T1 (3T3-hCycT1) cells expressing HIV-1 *gag, pol* genes (5×10^6 per 10-cm dish) were transfected using Lipofectamine 2000 with 10 μg of the pSM-SF162-env vector together with 5 μg of rev-expressing vector. Alternatively, replication-incompetent viruses were generated by transfection of 10 μg of VSV-G vector. The pseudotyped virus-containing culture supernatants of transfected cells were harvested at 48 h posttransfection. Supernatants were cleared of cellular debris by centrifugation at 500 *g* for 5 min and stored at −70°C, subsequent to a filtration through a 0.45-μm pore size filter and analyzed for HIV-1 p24 content by an enzyme-linked immunosorbent assay kit (ZeptoMetrix Corporation, Buffalo, NY). Virus pseudotyped by VSV-G was concentrated (141,000 *g* for 4 h at 4°C) and resuspended in a small amount of DMEM medium. A total of 10^6 target human osteosarcoma cells expressing both CD4 and CCR5 (HOShCD4hCCR5; Tahara-Hanaoka *et al.*, 2000) were plated on a 35-mm-diameter six-well culture plate and incubated with transfected cell media and 6 μg/ml of polybrene (Sigma Chemical Co., St. Louis, MO) for 3 h at 37°C, at which time 4 ml of complete medium was added and the incubation was continued. The medium was replaced 2 days later with medium containing 5 μg/ml of active puromycin for 10 days. The selection medium was changed every 2 to 3 days, and visible colonies arose typically in 6 to 9 days. These colonies were then stained with crystal violet.

Heterokaryon formation

Murine 3T3-hCycT1 cells (5×10^5) stably expressing HIV-1 *gag–pol* gene products were cocultured with an equal number of human HeLa, mink Mv.1.Lu, or murine NIH 3T3 cells in a culture plate (35-mm-diameter). After 12 h, medium was aspirated and the cells were washed once with serum-free medium. Then the cells were fused by adding 1.0 ml of a prewarmed 50% (wt/vol) polyethylene glycol [PEG (HYBRI-MAX; Sigma)] solution in DMEM for 2 min at 37°C. PEG was extensively washed, and heterokaryons were cultured for another 24 h. Culture supernatants was collected and the p24 CA content was monitored.

ACKNOWLEDGMENTS

We thank C. Cheng-Mayer for critical review of the manuscript and B. R. Cullen, R. Sutton, M. Hosokawa, and M. Sakaguchi for donating materials. We also thank K. Nishihara, T. Kimura, and T. Shimasaki for technical assistance; W. Song for assistance with confocal fluorescence microscopy; S. Shoji, K. Yoshimura, and Y. Kameyama for discussions; and M. Tsukiashi for secretarial services. This work was supported in part by a grant-in-aid for Scientific Research from the Ministry of Education of Japan.

REFERENCES

Atchison, R. E., Gosling, J., Monteclaro, F. S., Franci, C., Digilio, L., Charo, I. F., and Goldsmith, M. A. (1996). Multiple extracellular elements of CCR5 and HIV-1 entry: Dissociation from response to chemokines. *Science* **274,** 1924–1926.

Bieniasz, P. D., Grdina, T. A., Bogerd, H. P., and Cullen, B. R. (1998). Recruitment of a protein complex containing Tat and cyclin T1 to TAR governs the species specificity of HIV-1 Tat. *EMBO J.* **17,** 7056–7065.

Bieniasz, P. D., and Cullen, B. R. (2000). Multiple blocks to human immunodeficiency virus type 1 replication in rodent cells. *J. Virol.* **74,** 9868–9877.

Browning, J., Horner, J. W., Pettoello-Mantovani, M., Raker, C., Yurasov, S., DePinho, R. A., and Goldstein, H. (1997). Mice transgenic for human CD4 and CCR5 are susceptible to HIV infection. *Proc. Natl. Acad. Sci. UCA* **94,** 14637–14641.

Bryant, M., and Ratner, L. (1990). Myristoylation-dependent replication and assembly of human immunodeficiency virus 1. *Proc. Natl. Acad. Sci. USA* **87,** 523–527.

Canivet, M., Hoffman, A. D., Hardy, D., Sernatinger, J., and Levy, J. A. (1990). Replication of HIV-1 in a wide variety of animal cells following phenotypic mixing with murine retroviruses. *Virology* **178,** 543–551.

Chen, B. K., Rousso, I., Shim, S., and Kim, P. S. (2001). Efficient assembly of an HIV-1/MLV Gag-chimeric virus in murine cells. *Proc. Natl. Acad. Sci. USA* **98,** 15239–15244.

Clapham, P. R., Blanc, D., and Weiss, R. A. (1991). Specific cell surface requirements for the infection of CD4-positive cells by human immunodeficiency virus types 1 and 2 and by simian immunodeficiency virus. *Virology* **181,** 703–715.

Freed, E. O. (1998). HIV-1 gag proteins: Diverse functions in the virus life cycle. *Virology* **251,** 1–15.

Freed, E. O., Orenstein, J. M., Buckler-White, A. J., and Martin, M. A. (1994). Single amino acid changes in the human immunodeficiency virus type 1 matrix protein block virus particle production. *J. Virol.* **68,** 5311–5320.

Garber, M., Wei, P., KewalRamani, V., Mayall, T., Herrmann, C., Rice, A., Littman, D., and Jones, K. (1998). The interaction between HIV-1 Tat and human cyclin T1 requires zinc and a critical cysteine residue that is not conserved in the murine CycT1 protein. *Genes Dev.* **12,** 3512–3527.

Gheysen, D., Jacobs, E., de Foresta, F., Thiriart, C., Francotte, M., Thines, D., and De Wilde, D. (1989). Assembly and release of HIV-1 precursor Pr55gag virus-like particles from recombinant baculovirus-infected insect cells. *Cell* **59,** 103–112.

Gottlinger, H. G., Sodrosky, J. G., and Haseltine, W. A. (1989). Role of capsid precursor processing and myristoylation in morphogenesis and infectivity of human immunodeficiency virus. *Proc. Natl. Acad. Sci. USA* **86,** 5781–5785.

Hermida-Matsumoto, L., and Resh, M. D. (2000). Localization of human immunodeficiency virus type 1 Gag and Env at the plasma membrane by confocal imaging. *J. Virol.* **74,** 8670–8679.

Keppler, O. T., Welte, F. J., Ngo, T. A., Chin, P. S., Patton, K. S., Tsou, C.-L., Abbey, N. W., Sharkey, M. E., Grant, R. M., You, Y., Scarborough, J. D., Ellmeier, W., Littman, D. R., Stevenson, M., Charo, I. F., Herndier, B. G., Speck, R. F., and Goldsmith, M. A. (2002). Progress toward a human CD4/CCR5 transgenic rat model for de novo infection by human immunodeficiency virus type 1. *J. Exp. Med.* **195,** 719–736.

Koito, A., Harrowe, G., Levy, J. A., and Cheng-Mayer, C. (1994). Functional role of the V1/V2 region of human immunodeficiency virus type 1 envelope glycoprotein gp120 in infection of primary macrophages and sCD4 neutralization. *J. Virol.* **68,** 2253–2259.

Koito, A., Hattori, T., Matsushita, S., Maeda, Y., Nozaki, C., Sagawa, K., and Takatsuki, K. (1988). Conserved immunogenic region of a major core protein (p24) of human and simian immunodeficiency viruses. *AIDS Res. Hum. Retroviruses* **4,** 409–417.

Kwak, Y. T., Ivanov, D., Guo, J., Nee, E., and Gaynor, R. B. (1999). Role of the human and murine cyclin T proteins in regulating HIV-1 tat-activation. *J. Mol. Biol.* **288,** 57–69.

Leonard, J. M., Abramczuk, J. W., Pezen, D. S., Rutledge, R., Belcher, J. H., Hakim, F., Shearer, G., Lamperth, L., Travis, W., Fredrickson, T., Notkins, A. L., and Martin, M. A. (1988). Development of disease and virus recovery in transgenic mice containing HIV proviral DNA. *Science* **242,** 1665–1670.

Levy, J. A., Cheng-Mayer, C., Dina, D., and Luciw, P. A. (1986). AIDS retrovirus (ARV-2) clone replicates in transfected human and animal fibroblasts. *Science* **232,** 998–1001.

Lindwasser, O. W., and Resh, M. D. (2001). Multimerization of human immunodeficiency virus type 1 Gag promotes its localization to barges, raft-like membrane microdomains. *J. Virol.* **75,** 7913–7924.

Llopis, J., McCaffery, J. M., Miyawaki, A., Farquhar, M. G., and Tsien, R. Y. (1998). Measurement of cytosolic, mitochondrial, and Golgi pH in single living cells with green fluorescent proteins. *Proc. Natl. Acad. Sci. USA* **95,** 6803–6808.

Malim, M. H., McCarn, D. F., Tiley, L. S., and Cullen, B. R. (1991). Mutational definition of the human immunodeficiency virus type 1 Rev activation domain. *J. Virol.* **65,** 4248–4254.

Mariani, R., Rutter, G., Harris, M. E., Hope, T. J., Krausslich, H.-G., and Landau, N. R. (2000). A block to human immunodeficiency virus type 1 assembly in murine cells. *J. Virol.* **74,** 3859–3870.

Mariani, R., Rasala, B. A., Rutter, G., Wiegers, K., Brandt, S. M., Krausslich, H.-G., and Landau, N. R. (2001). Mouse-human heterokaryons support efficient human immunodeficiency virus type 1 assembly. *J. Virol.* **75,** 3141–3151.

Miller, A. D., and Rosman, G. J. (1989). Improved retroviral vectors for gene transfer and expression. *BioTechniques* **7,** 980–990.

Moosmayer, D., Reil, H., Ausmeier, M., Scharf, J.-G., Hauser, H., Jentsch, K. D., and Hunsmann, G. (1991). Expression and frameshifting but extremely inefficient proteolytic processing of the HIV-1 gag and pol gene products in stably transfected rodent cell lines. *Virology* **183,** 215–224.

Nguyen, D. H., and Hildreth, J. E. (2000). Evidence for budding of human immunodeficiency virus type 1 selectively from glycolipid-enriched membrane lipid rafts. *J. Virol.* **74,** 3264–3272.

Ono, A., and Freed, E. O. (2001). Plasma membrane rafts play a critical role in HIV-1 assembly and release. *Proc. Natl. Acad. Sci. USA* **98,** 13925–13930.

Ormo, M., Cubitt, A. B., Kallio, K., Gross, L. A., Tsien, R. Y., and Remington, S. J. (1996). Crystal structure of the *Aequorea victoria* green fluorescent protein. *Science* **273,** 1392–1395.

Reed, M., Mariani, R., Sheppard, L., Pekrun, K., Landau, N. R., and Soong, N.-W. (2002). Chimeric human immunodeficiency virus type 1 containing murine leukemia virus matrix assembles in murine cells. *J. Virol.* **76,** 436–443.

Rousso, I., Mixon, M. B., Chen, B. K., and Kim, P. S. (2000). Palmitoylation of the HIV-1 envelope glycoprotein is critical for viral infectivity. *Proc. Natl. Acad. Sci. USA* **97,** 13523–13525.

Sawada, S., Gowrishankar, K., Kitamura, R., Suzuki, M., Suzuki, G., Tahara, S., and Koito, A. (1998). Disturbed $CD4^+$ T cell homeostasis and *in vitro* susceptibility in transgenic mice expressing T cell line-tropic HIV-1 receptors. *J. Exp. Med.* **187,** 1439–1449.

Schnitzer, J. E., McIntosh, D. P., Dvorak, A. M., Liu, J., and Oh, P. (1995). Separation of caveolae from associated microdomains of GPI-anchored proteins. *Science* **269,** 1435–1439.

Shigekane, H., Kawaguchi, Y., Shirakata, M., Sakaguchi, M., and Hirai, K. (1999). The bi-directional transcriptional promoters for the latency-relating transcripts of the pp38/pp24 mRNAs and the 1.8 kb-mRNA in the long inverted repeats of Marek's disease virus serotype 1 DNA are regulated by common promoter-specific enhancers. *Arch. Virol.* **144,** 1893–1907.

Spearman, P., Horton, R., Ratner, L., and Kuli-Zade, I. (1997). Membrane binding of human immunodeficiency virus type 1 matrix protein *in vivo* supports a conformational myristyl switch mechanism. *J. Virol.* **71,** 6582–6592.

Tahara-Hanaoka, S., Ushijima, Y., Tarui, H., Wada, M., Hara, T., Imanishi, S., Yamaguchi, T., Hattori, T., Nakauchi, H., and Koito, A. (2000). Differential level in co-down-modulation of CD4 and CXCR4 primed by HIV-1 gp120 in response to phorbol ester, PMA, among HIV-1 isolates. *Microbiol. Immunol.* **44,** 489–498.

Wei, P., Garber, M. E., Fang, S. M., Fischer, W. H., and Jones, K. (1998). A novel CDK9-associated C-type cyclin interacts directly with HIV-1 Tat and mediates its high-affinity, loop-specific binding to TAR RNA. *Cell* **92,** 451–462.

Available online at www.sciencedirect.com
SCIENCE DIRECT®
Journal of Virological Methods 112 (2003) 121–128
Journal of Virological Methods
www.elsevier.com/locate/jviromet

The impact of highly active antiretroviral therapy by the oral route on the CD8 subset in monkeys infected chronically with $SHIV_{89.6P}$

Kazuhisa Yoshimura [a], Eiji Ido [c], Hisashi Akiyama [c], Tetsuya Kimura [a], Manabu Aoki [b], Hajime Suzuki [c], Hiroaki Mitsuya [b], Masanori Hayami [c], Shuzo Matsushita [a,*]

[a] *Division of Clinical Retrovirology and Infectious Diseases, Center for AIDS Research, Kumamoto University, 2-2-1 Honjo, Kumamoto 860-0811, Japan*
[b] *Department of Internal Medicine II, Kumamoto University, Kumamoto 860-0811, Japan*
[c] *The Laboratory of Viral Pathogenesis, Institute for Virus Research, Kyoto University, Kyoto 606-8507, Japan*

Received 27 March 2003; received in revised form 25 June 2003; accepted 26 June 2003

Abstract

The objective of this study was to assess the impact of highly active antiretroviral therapy (HAART) by an oral route on the peripheral blood CD8 subset in the monkeys infected persistently with a pathogenic strain, $SHIV_{89.6P}$. Two rhesus macaques were inoculated intravenously with $SHIV_{89.6P}$, then treated with the combination of AZT, 3TC and Lopinavir/Ritonavir (LPV/RTV) as recommended in humans by the oral route with confectionery continued for 28 days. In one of two chronically infected macaques, MM260, the viral load was maintained in the range of 10^4–10^5 copies/ml before HAART. The plasma viral load and proviral DNA decreased dramatically during the treatment, and cessation of this therapy the viral load rebounded to the pre-treatment level but the proviral DNA rebound was delayed. The other monkey, MM242, had low viral loads (1.2×10^3– $< 5 \times 10^2$ copies/ml) both before and after HAART. $CD4^+$ and $CD8^+$ T cell counts and proviral DNA level were not significantly changed after the treatment. The percentages of $CD8^+CD45RA^-Ki67^+$ cells increased during (MM260) or after (MM242) HAART and the subset was maintained at a high percentage until 18 weeks post HAART in MM242. These findings suggest that this primate model might serve an important role in testing the virological and immunological efficacy of novel therapeutic strategies combined with HAART.

Keywords: $SHIV_{89.6P}$; Antiretroviral therapy; $Ki67^+$; Memory $CD8^+$ T cells; Proviral DNA; Animal model

1. Introduction

Pre-clinical approaches in non-human primate models of AIDS enable pertinent evaluations to be carried out and the possibility to determine precisely the conditions of efficacy can be determined (Le Grand et al., 1994). Macaques infected with pathogenic strains of the simian immunodeficiency virus (SIV) or related chimeras expressing the envelope of HIV-1 (simian/human immunodeficiency virus, SHIV) are currently relevant models of human HIV infection and AIDS (Haigwood, 1999; Nath et al., 2000; Nathanson et al., 1999; Tang et al., 2002). SIV and SHIV have biological properties similar to those of HIV, and infection of macaques with pathogenic isolates induces an immunodeficiency syndrome strikingly mimicking human AIDS (Reimann et al., 1996a,b). Animal models are also useful for understanding the complexity of the pathogenic mechanisms of HIV infection during antiviral treatment (Endo et al., 2000; Enose et al., 2002; Igarashi et al., 2001).

SHIVs contain HIV-1-derived segments encoding viral envelope glycoproteins and regulatory proteins such as Tat, Rev and Vpu in the SIV background (Li et al., 1992). SHIV containing the envelope glycoproteins of a primary HIV-1 isolate, 89.6, replicated in rhesus monkeys but did not deplete $CD4^+$ T lymphocytes or induce disease in these animals. Serial transfer

* Corresponding author. Tel.: +81-96-373-6536; fax: +81-96-373-6537.
E-mail address: shuzo@kaiju.medic.kumamoto-u.ac.jp (S. Matsushita).

0166-0934/03/$ - see front matter © 2003 Elsevier B.V. All rights reserved.
doi:10.1016/S0166-0934(03)00201-5

of blood from $SHIV_{89.6}$-infected monkeys to naive monkeys generated a virus, termed $SHIV_{89.6P}$, that exhibited only a modest increase in replication in infected monkeys compared with $SHIV_{89.6}$. However, $SHIV_{89.6P}$ caused rapid loss of $CD4^+$ T lymphocytes and, subsequently, AIDS-like illness in inoculated monkeys (Reimann et al., 1996a,b). An animal system using $SHIV_{89.6P}$ acutely infected macaques with highly active antiretroviral therapy (HAART) was the same regimen used for humans (AZT+3TC+IDV) by the oral route (Le Grand et al., 2002, 2000; Thiebot et al., 2001) and a nasogastric catheter was placed for administering the drugs (Thiebot et al., 2001).

The objective of this study was to set up a novel AIDS model in monkeys and to evaluate the efficacy of the combination of AZT, 3TC and Lopinavir/Ritonavir (LPV/RTV), when administered by the oral route to the monkeys infected chronically with the pathogenic $SHIV_{89.6P}$.

2. Materials and methods

2.1. Cells and viruses

M8166 cells (Clapham et al., 1987) were grown in an RPMI-1640-based culture medium supplemented with 15% fetal calf serum (FCS: HyClone Laboratories, Logan, UT), 50 U/ml of penicillin and 50 mg/ml of streptomycin. $SHIV_{89.6P}$ (Reimann et al., 1996a) and $HIV\text{-}1_{LAI}$ (Clavel et al., 1986) were used for the drug susceptibility assay.

2.2. Antiviral agents

Zidovudine (AZT) was purchased from Sigma (St. Louis, MO). Lamivudine (3TC) was a kind gift from R.F. Schinazi (Atlanta, GA). RTV was kindly provided by Abbott Laboratories (Abbott Park, Ill.). LPV was synthesized using published methods (Carrillo et al., 1998). Kaletra™ liquid (LPV/RTV) and Combivir® tablets (AZT/3TC) were purchased from Abbott Laboratories and GlaxoSmithKline, respectively.

2.3. Drug susceptibility assay

The sensitivities of $SHIV_{89.6P}$ against various drugs were determined as described previously with minor modifications (Maeda et al., 2001; Yoshimura et al., 1999). Briefly, M8166 cells (5×10^3 per ml) were exposed to 100 $TCID_{50}$ of $SHIV_{89.6P}$ and $HIV\text{-}1_{LAI}$, in the presence of various concentrations of drugs in 96-well microculture plates and incubated at 37 °C for 7 days. After 100 μl of the medium was removed from each well, 10 μl of 3-(4,5-dimetylthiazol-2-yl)-2,5-diphenyltetrazolium bromide (MTT) solution (7.5 mg/ml) in phosphate-buffered saline (PBS) was added to each well in the plate, followed by incubation at 37 °C for 2 h. After incubation, to dissolve the formazan crystals, 100 μl of acidified isopropanol containing 4% (v/v) Triton X-100 was added to each well and the optical density was measured in a microplate reader. All assays were performed in duplicate (S.D.: $<25\%$).

2.4. Monkeys

Two rhesus macaques (*Macaca mulatta*), MM260 and MM242, were infected intravenously with 1000 and 10 $TCID_{50}$ (50% tissue culture infectious dose) of a pathogenic $SHIV_{89.6P}$, respectively. $SHIV_{89.6P}$ was provided by K.A. Reimann and N.L. Letvin (Beth Israel Hospital, Boston, MA). However, because the stock $SHIV_{89.6P}$, which was not the original virus used in this study might have slight loss of pathogenicity in the course of stock virus preparation, the CD4 values of the monkeys inoculated with $SHIV_{89.6P}$ sometimes showed a some reversal (20–50% of the mean value before inoculation) after the drastic drop up to 10% at 2–3 weeks post inoculation. The two animals were treated with a combination of AZT (5 mg/kg), 3TC (2.5 mg/kg) and LPV/RTV (12/3 mg/kg) administered by the oral route with confectionery twice a day after an intravenous inoculation of $SHIV_{89.6P}$. Briefly, Combivir tablets (AZT/3TC) were ground and mixed with Kaletra™ liquid (LPV/RTV) then the drug-mixture was poured into the sweet confectionery that the monkeys are fond of. We monitored the compliance of drug delivery by observing the monkeys until they had finished eating the sweets. Treatment was initiated 38 (MM260) or 84 (MM242) weeks after the inoculation of $SHIV_{89.6P}$, and was continued for 28 days. Two uninfected, untreated animals (MM132 and MM244) were used as controls (Fig. 3A and C). Blood samples were collected periodically from the infected and healthy macaques for analysis of $CD4^+$ and $CD8^+$ cell counts, $Ki67^+$ percentage, viral loads, and proviral DNA.

2.5. Measuring of proviral DNA level

Proviral DNA levels in peripheral blood mononuclear cells (PBMC) from $SHIV_{89.6P}$-infected-monkey were measured using a novel hypersensitive nested PCR in the LTR region. The first PCR was carried out with SHIV-O-S (5′-AGGCATCATACCAGATTGGCA-3′) and SHIV-O-A (5′-ATTGAAGAGGGCTTTAAGCAA-3′) primers in the U3/R region. The first PCR reaction mixture consisted of 0.5 μg of the proviral DNA solution, 50 mM KCl, 10 mM Tris–HCl (pH 8.0), 2 mM $MgCl_2$, 0.01% gelatin, 0.2 mM dNTPs, 1.5 U of EX Taq DNA polymerase (Takara Shuzo Co., LTD.), and 15 pmol of each of the first PCR primers in a total volume of 30 μl. The PCR conditions used were an

initial 3 min at 94 °C, followed by 24 cycles of 30 s at 94 °C, 30 s at 65 °C, and 1 min at 70 °C with a final 10 min extension at 72 °C. The first PCR product was subsequently diluted 1000-fold, and subjected to a real-time PCR assay for measuring U3 DNA using SHIV-I-S (5′-AGACATTTGGCTGGCTATGGA-3′), SHIV-I-A (5′-AAGTTTGAGCTGGATGCATTA-3′) and SYBR Green PCR Master Mix (Perkin–Elmer-Applied Biosystems). For amplification and detection of PCR products we preheated the samples at 50 °C for 2 min and at 95 °C for 10 min, followed by 40 cycles of denaturation at 95 °C for 15 s and annealing/extension at 60 °C for 30 s, using an ABI PRISM 7700 sequence detection system (Perkin–Elmer-Applied Biosystems). The SIVmac239 LTR sequence was cloned into pCR2.1 TOPO vector (Invitrogen), and served as a standard curve. The level of SHIV DNA was expressed as copies per micrograms of cellular DNA (copies/μg DNA). Under these conditions, the detection limit was 300 copies/μg DNA.

2.6. Detection of plasma viral RNA

Plasma viral loads were determined using Taqman RT-PCR kits (Perkin–Elmer, New Jersey, USA) and ABI Prism 7700 (Ui et al., 1999). Absolute copy numbers of viral RNAs were determined using standard plasma samples, the copy numbers, of which were determined by Chiron Corporation. Under these conditions, the detection limit was 500 copies/ml.

2.7. FACS analysis

Whole blood samples of the monkeys were stained with fluorecently labeled mouse monoclonal antibodies as follows; phycoerythrin (PE)-conjugated anti-human CD4 (NU-$T_{H/N}$, Nichirei, Japan), PerCP-conjugated anti-human CD8 monoclonal antibody (Leu-2a, BD PharMingen, CA). After hemolysis of the blood using a lysing solution (BD PharMingen), the, respectively, labeled lymphocytes were analyzed using FACSCalibur (BD PharMingen).

PBMCs were also isolated from the macaques using centrifugation on Ficoll–Hypaque density gradient centrifugation. The PBMCs were incubated with fluorochrome-labeled specific monoclonal antibodies against surface antigens, allophycocyanin (APC)-conjugated anti-human CD8 (RPA-T8, BD PharMingen) and PE-conjugated anti-human CD45RA (5H9, BD PharMingen), and also incubated with 7-amino-actinomycin D (7-AAD) (BD PharMingen) to exclude dead cells. After fixation and permeabilization, the cells were incubated with Ki67-FITC (B56, BD PharMingen). The stained cells were analyzed by four-color flow cytometry using a FACSCalibur (Kimura et al., 2002).

2.8. Statistical analysis

The $CD4^+$ and $CD8^+$ T cell counts between pre-HAART and baseline or post-HAART were determined statistically using Student's t-test.

3. Results

3.1. In vitro drug sensitivity of $SHIV_{89.6P}$ and HIV-1_{LAI}

We first tested two nucleoside reverse transcriptase inhibitors (NRTIs), AZT and 3TC, and two protease inhibitors (PIs), RTV and LPV, against $SHIV_{89.6P}$ and HIV-1_{LAI} in M8166 cells (Table 1). Antiviral activity of the two NRTIs was comparable against these two viruses. On the other hand, as shown in Table 1, $SHIV_{89.6P}$ had a high level of resistance to RTV (15–18-fold increase in IC_{50}) and a moderate level of resistance to LPV (5–6-fold) compared with the case against HIV-1_{LAI}. This finding is similar to a pattern of sensitivity of HIV-2 strains to PIs as reported (Yoshimura et al., 1999).

3.2. $SHIV_{89.6P}$-infected macaques were treated with HAART by the oral route

The replication of $SHIV_{89.6P}$ was inhibited by AZT, 3TC or LPV within the IC_{50} range between 0.007 and 0.47 μM in vitro (Table 1). We selected these three drugs for treatment to monkeys infected with $SHIV_{89.6P}$ because this combination is currently recommended for treatment of patients with HIV-1 infection. Two rhesus macaques were inoculated intravenously with 1000 and 10 $TCID_{50}$ of a cell-free stock of $SHIV_{89.6P}$ for MM260 and MM242, respectively. The monkeys, MM260 and MM242, became infected and were treated with HAART initiated at 38 and 64 weeks and continued until at 42 and 68 weeks post-inoculation, respectively. The animals were treated, as recommended in the case of humans, by the combination of AZT (5 mg/kg bid), 3TC (2.5 mg/kg bid) and LPV/RTV (12/3 mg/kg bid) after the intravenous inoculation of $SHIV_{89.6P}$. This treatment was administered by the oral route together with confectionery and was continued for 28 days. The animals (MM260 and MM242) were monitored for $CD4^+$ and $CD8^+$ T cell counts, viral loads in plasma, proviral DNA and $CD8^+$ T cell turnover.

MM260, the monkey with the high viral load showed a significant decline in $CD4^+$ but not $CD8^+$ T cell counts before HAART compared with the pre-infection level (598 ± 80 vs. 49 ± 16 per μl in mean $CD4^+$ count ± S.D., $P < 0.001$ determined by the Student's t-test, 288 ± 46 vs. 221 ± 81 per μl in mean $CD8^+$ count ± S.D., $P = 0.25$). $CD4^+$ and $CD8^+$ T cell counts

Table 1
Sensitivities of $SHIV_{89.6P}$ and $HIV\text{-}1_{LAI}$ to RTIs (AZT and 3TC) and PIs (LPV and RTV)

Virus	Cells	IC_{50} (μM) ± S.D.s[a]			
		AZT	3TC	LPV	RTV
$SHIV_{89.6P}$	M8166	0.007 ± 0.002	0.43 ± 0.0001	0.47 ± 0.09	0.44 ± 0.07
$HIV\text{-}1_{LAI}$	M8166	0.013 ± 0.001	0.31 ± 0.15	0.08 ± 0.01	0.03 ± 0.004

RTIs, reverse transcriptase inhibitors; AZT, zidovudine; 3TC, lamivudine. PIs, protease inhibitors; LPV, lopinavir; RTV, ritonavir.
[a] Data shown represent mean values (with standard deviations) derived from the result of two independent experiments conducted in duplicate. M8166 cells (5×10^3) were exposed to 100 $TCID_{50}$ of $SHIV_{89.6P}$ or $HIV\text{-}1_{LAI}$ caltured in the presence of various concentrations of RTIs or PIs, and IC_{50}s were determined using the MTT assay on day 7 of culture.

increased during and after treatment compared with the pre-HAART level (49 ± 16 vs. 99 ± 26 per μl in mean $CD4^+$ count ± S.D., $P = 0.002$, 221 ± 81 vs. 392 ± 108 per μl in mean $CD8^+$ count ± S.D., $P = 0.01$) (Fig. 1A). At week 38, when HAART was initiated, the plasma viral load in MM260 was 3.4×10^4 copies/ml, and the proviral DNA was 6.8×10^4 copies/μg DNA. After commencement of HAART, the viral RNA in the plasma declined to below the threshold of detection within 3 weeks post HAART. On the other hand, proviral DNA remained detectable under the treatment though a continuous decline in the level was observed at 9 weeks post HAART (Fig. 1B).

In the low viral load monkey, MM242, the $CD4^+$ cell numbers were maintained over 400 per μl before HAART but the macaque also showed a decline in $CD4^+$ but not $CD8^+$ T cell counts before HAART compared with the pre-infection level (2152 ± 542 vs.

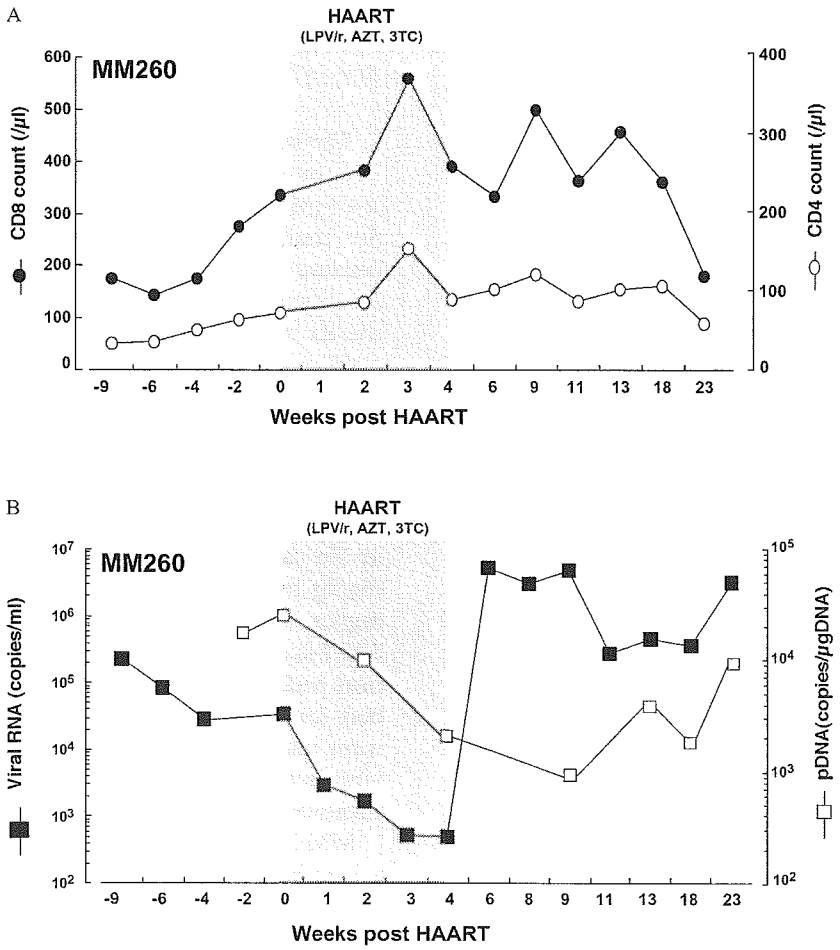

Fig. 1. Analyses of $SHIV_{89.6P}$-infected rhesus macaque MM260 treated with LPV/r, AZT and 3TC for 4 weeks by the oral route. $CD4^+$ and $CD8^+$ T cell counts (A), and plasma viral load and proviral DNA copy number (B) assessed within the peripheral blood are shown. The treatment period is shaded.

577 ± 139 per μl in mean $CD4^+$ count ± S.D., $P < 0.001$, 761 ± 248 vs. 447 ± 188 per μl in mean $CD8^+$ count ± S.D., $P = 0.09$). However, there was no significant difference between pre- and after HAART in $CD4^+$ and $CD8^+$ T cell counts (577 ± 139 vs. 569 ± 180 per μl in mean $CD4^+$ count ± S.D., $P = 0.93$, 447 ± 188 vs. 385 ± 159 per μl in mean $CD8^+$ count ± S.D., $P = 0.52$) (Fig. 2A). The plasma viral load in MM242 was detectable at one point (9 weeks before HAART) before the treatment, and was never detected during and after treatment. The proviral DNAs in MM242 were also low (< 300–1590 copies/μg DNA), and was maintained below the threshold of detection after the discontinuation of HAART (Fig. 2B).

3.3. Analysis of $CD8^+Ki67^+$ T cells in $SHIV_{89.6P}$-infected macaques with HAART

We determined Ki67-positive $CD8^+$ T cells in $SHIV_{89.6P}$-infected and uninfected monkeys using four-color flow cytometry analysis (Sachsenberg et al., 1998; Sodora et al., 2002). In the $SHIV_{89.6P}$-infected animal with a high viral load, MM260, growth fraction (percentage of Ki67) of $CD8^+$ T cells (10.98%) before HAART was higher than the value in the uninfected monkey (1.07%). The Ki67-positive $CD8^+$ T cells in MM260 were increasing during HAART, especially in the $CD45RA^-$ (CD8 memory) subset. After the discontinuation of HAART, the percentage of $CD8^+Ki67^+$ subset declined to the pre-treatment level (Fig. 3A and B). In MM242, the percentage of $CD8^+Ki67^+$ subset at 4 weeks before HAART was comparable to that of the uninfected monkey (0.83 vs. 0.85%). Ki67 levels were elevated after the treatment and were maintained at a high level until 18 weeks post HAART (7.95%). $CD8^+CD45RA^+Ki67^+$ T cells in MM242 increased after HAART, however, the $CD8^+CD45RA^-Ki67^+$ T cells were also increasing and overcame the percentage of $CD8^+CD45RA^+Ki67^+$ T cells by 13 weeks post HAART (Fig. 3C and D). We also determined Ki67 positivity in $CD8^+CD56^+$ T cells in MM242 at pre- and post-HAART. The percentages of $CD56^+Ki67^+$ were 0% and 0.05% in the $CD8^+$ T cell population at pre- (−3 weeks) and post- (22 weeks) HAART, respectively, using flow cytometry analysis. There

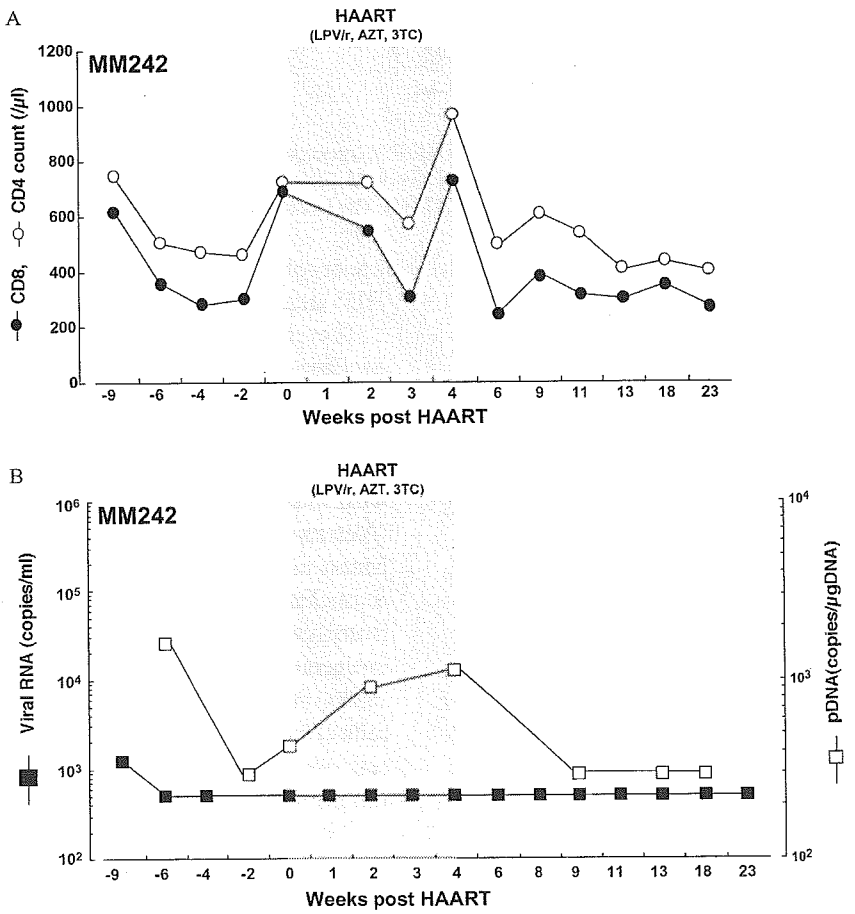

Fig. 2. Analyses of $SHIV_{89.6P}$-infected rhesus macaque MM242 treated with LPV/r, AZT and 3TC for 4 weeks by the oral route. $CD4^+$ and $CD8^+$ T cell counts (A), and plasma viral load and proviral DNA copy number (B) assessed within the peripheral blood are shown. The treatment period is shaded.

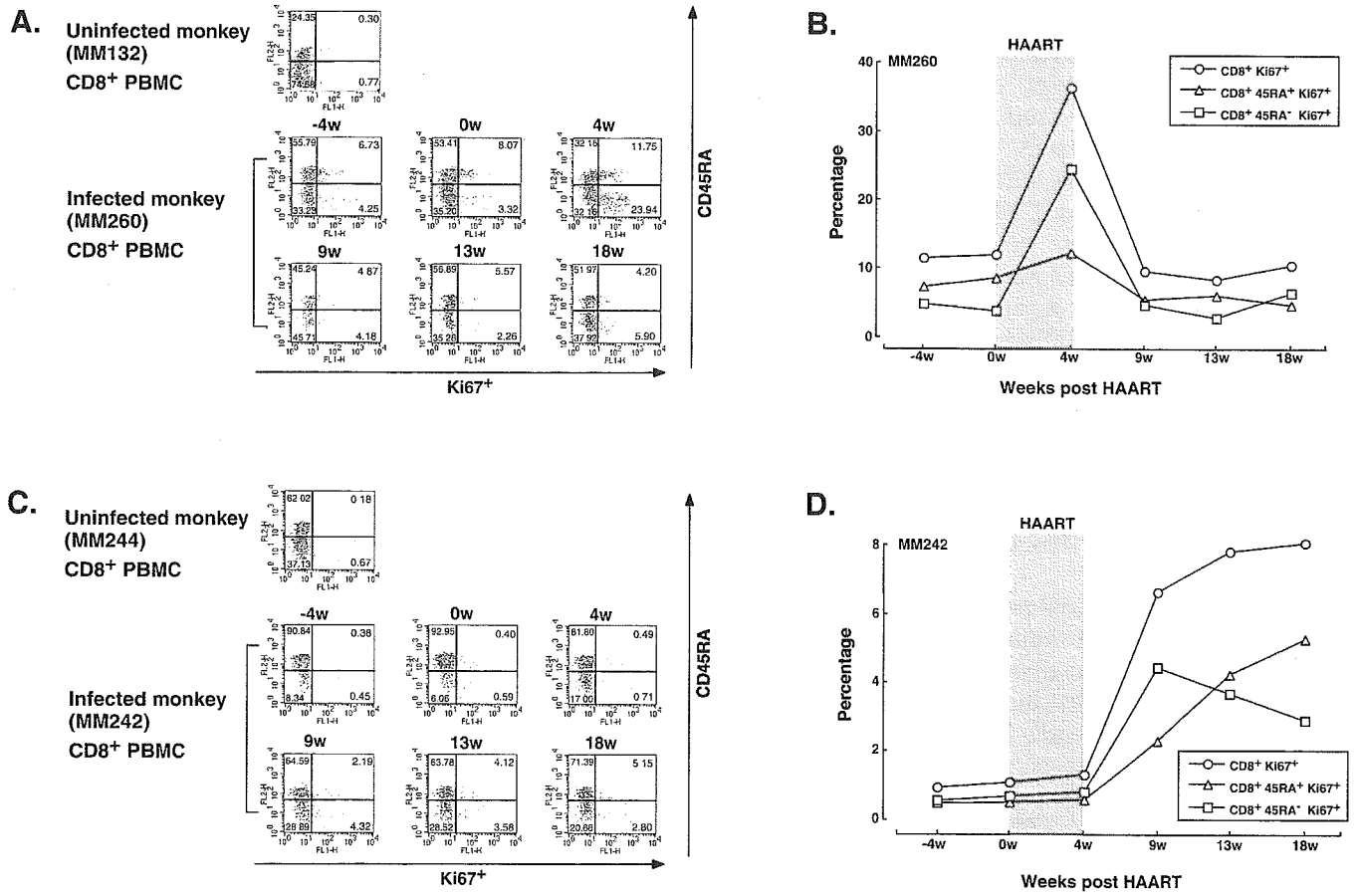

Fig. 3. Flow cytometry analysis of $CD8^+CD45RA^+$ cells stained with Ki-67. Expression of Ki-67 (percentage) in $CD8^+$ T cells of a control monkey and a $SHIV_{89.6P}$-infected monkey MM260 (A) and MM242 (C) at −4, 0, 4, 9, 13, 18 weeks post HAART. The percentage of cells expressing Ki-67 and CD45RA in $CD8^+$ T cells is depicted for MM260 (B) and MM242 (D). The treatment period is shaded.

seemed to be little contribution of $CD8^+$ NK cells in our data on $CD8^+Ki67^+$ T cells.

4. Discussion

This is apparently the first demonstration that the model of chronically $SHIV_{89.6P}$ infected-monkey with a therapeutic design recommended for humans by the oral route is feasible. The reduction of viral load and proviral DNA during the chronically infected stage was observed in treated animals together with the increase of CD4 and CD8 positive T lymphocyte subsets, especially memory T cells. Moreover, in both macaques, the percentages of $CD8^+Ki67^+$ cells increased during HAART, especially in the low viral load monkey (MM242) and the subset was maintained at a high percentage until 18 weeks post HAART. In CD4 positive T cells, $Ki67^+$ cells were also increased until 18 weeks post HAART in MM242 (data not shown). These results suggest that the oral treatment system in chronically infected-monkeys may prove to be a useful tool for monitoring immunological changes undergoing novel antiviral strategies with the usual anti-HIV treatment regimen.

The recent use of HAART has indicated that the decline of viral load in plasma and tissues generally results in an increase of T cell counts in peripheral blood (Autran et al., 1997; Evans et al., 1998; Mezzaroma et al., 1999; Pakker et al., 1998), which is often associated with improvement in clinical and immunological status (Autran et al., 1997; Evans et al., 1998). The mechanism(s) involved in such a peripheral T cell repopulation is unclear and may reflect the contribution of T cells from lymphoid tissues as a consequence of the reduced antigenic stimulation (Autran et al., 1997; Pakker et al., 1998), the capability for de novo production of naïve T cells (Hellerstein et al., 1999), and a decreased rate of T cell loss, which may reflect a reduced T cell susceptibility to apoptotic stimuli (Gougeon et al., 1999).

The issue of T lymphocyte turnover is central to understanding of HIV-1 pathogenesis (Antia and Halloran, 1996). Sachsenberg et al. estimated that HIV-1-infected individuals had a mean 6-fold increase in $CD8^+$T cell turnover, whereas the mean turnover of $CD4^+$T cells only increased by 2-fold (Sachsenberg et

al., 1998). The higher turnover of $CD8^+$ T cells reflects the inversion of the $CD4^+/CD8^+$ ratio in HIV-1-infected patients (Chun et al., 2002; Margolick et al., 1995). In those studies, differences in $CD4^+$ and $CD8^+$ T cell turnover also depend on stage of the disease, as defined by $CD4^+$ T cell counts.

$CD8^+$ T cell counts and the percentage of $CD8^+CD45RA^-$ (memory) T cells in both chronically infected macaques increased after oral route treatment. These findings were usually seen in clinical cases at the beginning of HAART (Autran et al., 1997; Badley et al., 1999; Pakker et al., 1998). However, the majority of $CD8^+$ memory cells increased following HAART was not considered as HIV-specific T cells. Because levels of HIV-specific effect CTL in treatment individuals fell (median half-life, 45 days) while viral RNA remained undetectable (Ogg et al., 1999). It is conceivable that following HAART reduction of apoptosis in $CD8^+$ memory cells may lead to an increase in the population. Our finding in infected monkeys with HAART was very similar to the kinetic of $CD8^+$ T cells after treatment of humans. The experiment presented in this report may provide an animal model of the phenomenon observed in HIV infected patients. Further analysis of repopulated $CD8^+$ T cells would be of interest because HIV-1 specific $CD8^+$ T cells during chronic infection in humans are enriched in cells of the $CD28^-CD27^+$ phenotype that proliferate but do have reduced CTL activity (Appay et al., 2002). Whether or not the proliferating $CD8^+$ T cells in our macaques given HAART are cells of this phenotype will need to be determined.

The plasma HIV-1 RNA is widely considered to be a direct indicator of the overall level of HIV-1 expression in infected individuals. However, it was reported that the concentration of HIV-1 DNA in PBMC complements the HIV-1 RNA load in plasma in predicting the clinical outcome of HIV-1 disease (Kostrikis et al., 2002). In our findings, especially in MM242 with a low plasma $SHIV_{89.6P}$ RNA load, the proviral DNA also may be an indicator of residual replication when plasma RNA loads were undetectable as seen in HIV-1 infected patients (Kostrikis et al., 2002; O'Doherty et al., 2002).

These monkey model given antiviral drugs by the oral route will enable the investigation of immunological changes during novel drug testing and also antiviral strategies combined with HAART.

Acknowledgements

We thank K. Yoshida and N. Shirai for excellent technical assistance and Dr A. Koito for helpful comments on the manuscript. This work was supported in part by Research for Scientific Research Grant of the Japan Society for the Promotion of Science (#14021099), a Grant-in-Aid for Scientific Research (Priority Areas) from the Ministry of Education, Culture, Sports, Science, and Technology of Japan (Monbu-Kagakusho)(#14570422).

References

Antia, R., Halloran, M.E., 1996. Recent developments in theories of pathogenesis of AIDS. Trends Microbiol. 4 (7), 282–285.

Appay, V., Dunbar, P.R., Callan, M., Klenerman, P., Gillespie, G.M., Papagno, L., Ogg, G.S., King, A., Lechner, F., Spina, C.A., Little, S., Havlir, D.V., Richman, D.D., Gruener, N., Pape, G., Waters, A., Easterbrook, P., Salio, M., Cerundolo, V., McMichael, A.J., Rowland-Jones, S.L., 2002. Memory $CD8^+$ T cells vary in differentiation phenotype in different persistent virus infections. Nat. Med. 8 (4), 379–385.

Autran, B., Carcelain, G., Li, T.S., Blanc, C., Mathez, D., Tubiana, R., Katlama, C., Debre, P., Leibowitch, J., 1997. Positive effects of combined antiretroviral therapy on $CD4^+$ T cell homeostasis and function in advanced HIV disease. Science 277 (5322), 112–116.

Badley, A.D., Parato, K., Cameron, D.W., Kravcik, S., Phenix, B.N., Ashby, D., Kumar, A., Lynch, D.H., Tschopp, J., Angel, J.B., 1999. Dynamic correlation of apoptosis and immune activation during treatment of HIV infection. Cell Death Differ. 6 (5), 420–432.

Carrillo, A., Stewart, K.D., Sham, H.L., Norbeck, D.W., Kohlbrenner, W.E., Leonard, J.M., Kempf, D.J., Molla, A., 1998. In vitro selection and characterization of human immunodeficiency virus type 1 variants with increased resistance to ABT-378, a novel protease inhibitor. J. Virol. 72 (9), 7532–7541.

Chun, T.W., Justement, J.S., Pandya, P., Hallahan, C.W., McLaughlin, M., Liu, S., Ehler, L.A., Kovacs, C., Fauci, A.S., 2002. Relationship between the size of the human immunodeficiency virus type 1 (HIV-1) reservoir in peripheral blood $CD4^+$ T cells and $CD4^+$:$CD8^+$ T cell ratios in aviremic HIV-1-infected individuals receiving long-term highly active antiretroviral therapy. J. Infect. Dis. 185 (11), 1672–1676.

Clapham, P.R., Weiss, R.A., Dalgleish, A.G., Exley, M., Whitby, D., Hogg, N., 1987. Human immunodeficiency virus infection of monocytic and T-lymphocytic cells: receptor modulation and differentiation induced by phorbol ester. Virology 158 (1), 44–51.

Clavel, F., Guetard, D., Brun-vezinet, F., Chamaret, S., Rey, M.A., Santos-ferreira, M.O., Laurent, A.G., Dauguet, C., Katlama, C., Rouzioux, C., 1986. Isolation of a new human retrovirus from West African patients with AIDS. Science 233 (4761), 343–346.

Endo, Y., Igarashi, T., Nishimura, Y., Buckler, C., Buckler-White, A., Plishka, R., Dimitrov, D.S., Martin, M.A., 2000. Short- and long-term clinical outcomes in rhesus monkeys inoculated with a highly pathogenic chimeric simian/human immunodeficiency virus. J. Virol. 74 (15), 6935–6945.

Enose, Y., Ui, M., Miyake, A., Suzuki, H., Uesaka, H., Kuwata, T., Kunisawa, J., Kiyono, H., Takahashi, H., Miura, T., Hayami, M., 2002. Protection by intranasal immunization of a nef-deleted, nonpathogenic SHIV against intravaginal challenge with a heterologous pathogenic SHIV. Virology 298 (2), 306–316.

Evans, T.G., Bonnez, W., Soucier, H.R., Fitzgerald, T., Gibbons, D.C., Reichman, R.C., 1998. Highly active antiretroviral therapy results in a decrease in $CD8^+$ T cell activation and preferential reconstitution of the peripheral $CD4^+$ T cell population with memory rather than naive cells. Antiviral Res. 39 (3), 163–173.

Gougeon, M.L., Lecoeur, H., Sasaki, Y., 1999. Apoptosis and the CD95 system in HIV disease: impact of highly active anti-retroviral therapy (HAART). Immunol. Lett. 66 (1–3), 97–103.

Haigwood, N.L., 1999. Progress and challenges in therapies for AIDS in nonhuman primate models. J. Med. Primatol. 28 (4–5), 154–163.

Hellerstein, M., Hanley, M.B., Cesar, D., Siler, S., Papageorgopoulos, C., Wieder, E., Schmidt, D., Hoh, R., Neese, R., Macallan, D., Deeks, S., McCune, J.M., 1999. Directly measured kinetics of circulating T lymphocytes in normal and HIV-1-infected humans. Nat. Med. 5 (1), 83–89.

Igarashi, T., Brown, C.R., Endo, Y., Buckler-White, A., Plishka, R., Bischofberger, N., Hirsch, V., Martin, M.A., 2001. Macrophage are the principal reservoir and sustain high virus loads in rhesus macaques after the depletion of $CD4^+$ T cells by a highly pathogenic simian immunodeficiency virus/HIV type 1 chimera (SHIV): implications for HIV-1 infections of humans. Proc. Natl. Acad. Sci. USA 98 (2), 658–663.

Kimura, T., Yoshimura, K., Nishihara, K., Maeda, Y., Matsumi, S., Koito, A., Matsushita, S., 2002. Reconstitution of spontaneous neutralizing antibody response against autologous human immunodeficiency virus during highly active antiretroviral therapy. J. Infect. Dis. 185 (1), 53–60.

Kostrikis, L.G., Touloumi, G., Karanicolas, R., Pantazis, N., Anastassopoulou, C., Karafoulidou, A., Goedert, J.J., Hatzakis, A., 2002. Quantitation of human immunodeficiency virus type 1 DNA forms with the second template switch in peripheral blood cells predicts disease progression independently of plasma RNA load. J. Virol. 76 (20), 10099–10108.

Le Grand, R., Clayette, P., Noack, O., Vaslin, B., Theodoro, F., Michel, G., Roques, P., Dormont, D., 1994. An animal model for antilentiviral therapy: effect of zidovudine on viral load during acute infection after exposure of macaques to simian immunodeficiency virus. AIDS Res. Hum. Retroviruses 10 (10), 1279–1287.

Le Grand, R., Vaslin, B., Larghero, J., Neidez, O., Thiebot, H., Sellier, P., Clayette, P., Dereuddre-Bosquet, N., Dormont, D., 2000. Post-exposure prophylaxis with highly active antiretroviral therapy could not protect macaques from infection with SIV/HIV chimera. AIDS 14 (12), 1864–1866.

Le Grand, R., Vaslin, B., Benlhassan, K., Thiebot, H., Dereuddre-Bosquet, N., Clayette, P., Dormont, D., 2002. Post-exposure prophylaxis with HAART in macaques exposed to pathogenic SIV or SHIV. XIV International AIDS Conference.

Li, J., Lord, C.I., Haseltine, W., Letvin, N.L., Sodroski, J., 1992. Infection of cynomolgus monkeys with a chimeric HIV-1/SIVmac virus that expresses the HIV-1 envelope glycoproteins. J. Acquired Immune Defic. Syndr. 5 (7), 639–646.

Maeda, K., Yoshimura, K., Shibayama, S., Habashita, H., Tada, H., Sagawa, K., Miyakawa, T., Aoki, M., Fukushima, D., Mitsuya, H., 2001. Novel low molecular weight spirodiketopiperazine derivatives potently inhibit R5 HIV-1 infection through their antagonistic effects on CCR5. J. Biol. Chem. 276 (37), 35194–35200.

Margolick, J.B., Munoz, A., Donnenberg, A.D., Park, L.P., Galai, N., Giorgi, J.V., O'Gorman, M.R., Ferbas, J., 1995. Failure of T-cell homeostasis preceding AIDS in HIV-1 infection. The Multicenter AIDS Cohort Study. Nat. Med. 1 (7), 674–680.

Mezzaroma, I., Carlesimo, M., Pinter, E., Alario, C., Sacco, G., Muratori, D.S., Bernardi, M.L., Paganelli, R., Aiuti, F., 1999. Long-term evaluation of T-cell subsets and T-cell function after HAART in advanced stage HIV-1 disease. AIDS 13 (10), 1187–1193.

Nath, B.M., Schumann, K.E., Boyer, J.D., 2000. The chimpanzee and other non-human-primate models in HIV-1 vaccine research. Trends Microbiol. 8 (9), 426–431.

Nathanson, N., Hirsch, V.M., Mathieson, B.J., 1999. The role of nonhuman primates in the development of an AIDS vaccine. AIDS 13 (Suppl. A), S113–S120.

O'Doherty, U., Swiggard, W.J., Jeyakumar, D., McGain, D., Malim, M.H., 2002. A sensitive, quantitative assay for human immunodeficiency virus type 1 integration. J. Virol. 76 (21), 10942–10950.

Ogg, G.S., Jin, X., Bonhoeffer, S., Moss, P., Nowak, M.A., Monard, S., Segal, J.P., Cao, Y., Rowland-Jones, S.L., Hurley, A., Markowitz, M., Ho, D.D., McMichael, A.J., Nixon, D.F., 1999. Decay kinetics of human immunodeficiency virus-specific effector cytotoxic T lymphocytes after combination antiretroviral therapy. J. Virol. 73 (1), 797–800.

Pakker, N.G., Notermans, D.W., de Boer, R.J., Roos, M.T., de Wolf, F., Hill, A., Leonard, J.M., Danner, S.A., Miedema, F., Schellekens, P.T., 1998. Biphasic kinetics of peripheral blood T cells after triple combination therapy in HIV-1 infection: a composite of redistribution and proliferation. Nat. Med. 4 (2), 208–214.

Reimann, K.A., Li, J.T., Veazey, R., Halloran, M., Park, I.W., Karlsson, G.B., Sodroski, J., Letvin, N.L., 1996a. A chimeric simian/human immunodeficiency virus expressing a primary patient human immunodeficiency virus type 1 isolate env causes an AIDS- like disease after in vivo passage in rhesus monkeys. J. Virol. 70 (10), 6922–6928.

Reimann, K.A., Li, J.T., Voss, G., Lekutis, C., Tenner-Racz, K., Racz, P., Lin, W., Montefiori, D.C., Lee-Parritz, D.E., Lu, Y., Collman, R.G., Sodroski, J., Letvin, N.L., 1996b. An env gene derived from a primary human immunodeficiency virus type 1 isolate confers high in vivo replicative capacity to a chimeric simian/human immunodeficiency virus in rhesus monkeys. J. Virol. 70 (5), 3198–3206.

Sachsenberg, N., Perelson, A.S., Yerly, S., Schockmel, G.A., Leduc, D., Hirschel, B., Perrin, L., 1998. Turnover of $CD4^+$ and $CD8^+$ T lymphocytes in HIV-1 infection as measured by Ki-67 antigen. J. Exp. Med. 187 (8), 1295–1303.

Sodora, D.L., Milush, J.M., Ware, F., Wozniakowski, A., Montgomery, L., McClure, H.M., Lackner, A.A., Marthas, M., Hirsch, V., Johnson, R.P., Douek, D.C., Koup, R.A., 2002. Decreased levels of recent thymic emigrants in peripheral blood of simian immunodeficiency virus-infected macaques correlate with alterations within the thymus. J. Virol. 76 (19), 9981–9990.

Tang, Y., Villinger, F., Staprans, S.I., Amara, R.R., Smith, J.M., Herndon, J.G., Robinson, H.L., 2002. Slowly declining levels of viral RNA and DNA in DNA/recombinant modified vaccinia virus Ankara-vaccinated macaques with controlled simian-human immunodeficiency virus SHIV-89.6P challenges. J. Virol. 76 (20), 10147–10154.

Thiebot, H., Louache, F., Vaslin, B., de Revel, T., Neildez, O., Larghero, J., Vainchenker, W., Dormont, D., Le Grand, R., 2001. Early and persistent bone marrow hematopoiesis defect in simian/human immunodeficiency virus-infected macaques despite efficient reduction of viremia by highly active antiretroviral therapy during primary infection. J. Virol. 75 (23), 11594–11602.

Ui, M., Kuwata, T., Igarashi, T., Ibuki, K., Miyazaki, Y., Kozyrev, I.L., Enose, Y., Shimada, T., Uesaka, H., Yamamoto, H., Miura, T., Hayami, M., 1999. Protection of macaques against a SHIV with a homologous HIV-1 Env and a pathogenic SHIV-89.6P with a heterologous Env by vaccination with multiple gene-deleted SHIVs. Virology 265 (2), 252–263.

Yoshimura, K., Kato, R., Yusa, K., Kavlick, M.F., Maroun, V., Nguyen, A., Mimoto, T., Ueno, T., Shintani, M., Falloon, J., Masur, H., Hayashi, H., Erickson, J., Mitsuya, H., 1999. JE-2147: a dipeptide protease inhibitor (PI) that potently inhibits multi-PI-resistant HIV-1. Proc. Natl. Acad. Sci. USA 96 (15), 8675–8680.

ELSEVIER

Journal of Clinical Virology 33 (2005) 188–193

JOURNAL OF CLINICAL VIROLOGY

www.elsevier.com/locate/jcv

Spontaneous recovery of hemoglobin and neutrophil levels in Japanese patients on a long-term Combivir® containing regimen

Shuzo Matsushita[a,d,*], Kazuhisa Yoshimura[a,d], Tetsuya Kimura[a], Asako Kamihira[b], Misao Takano[c], Kenichiro Eto[d], Takuma Shirasaka[b], Hiroaki Mitsuya[d], Shinichi Oka[c]

[a] *Division of Clinical Retrovirology and Infectious Diseases, Center for AIDS Research, Kumamoto University, 2-2-1 Honjo, Kumamoto 860-0811, Japan*
[b] *Department of Immunological and Infectious Diseases, Osaka National Hospital, Osaka 540-0006, Japan*
[c] *AIDS Clinical Center, International Medical Center of Japan, Tokyo 162-8655, Japan*
[d] *Department of Infectious Diseases, Kumamoto University School of Medicine, Kumamoto 860-8556, Japan*

Received 11 August 2004; accepted 3 November 2004

Abstract

Objective: In order to evaluate long-term toxicity of Combivir, we retrospectively reviewed clinical records of HIV-1 infected cases under treatment with Combivir-containing regimen and we analyzed the clinical data compared to other NRTIs-containing regimens.
Study design: A total of 55 patients who were on Combivir and 39 on a control regimen were examined.
Results: After starting treatment with Combivir-containing regimens viral load and $CD4^+$ T-cell count improved as well as the control group. Rates of adverse events in Combivir group and ZDV (400 mg/day) + 3TC group were 50.9% (28/55) and 60% (12/20), respectively. Some of these Japanese patients who started Combivir regimen as a first-line HAART (primary Combivir group) showed some decrease in hemoglobin levels or neutrophil counts within 6 months. However, a significant recovery of these indices of hematological toxicities occurred in patients who continued the regimen for 18–24 months.
Conclusion: Our findings suggest that the safety of 600 mg of ZDV is similar to 400 mg/day of ZDV and the existence of mechanisms that compensate for anemia and for the neutropenia associated with long-term use of Combivir.

Keywords: Combivir; Zidovudine; Lamivudine; Hemoglobin; Neutrophil; Long-term treatment

1. Introduction

Prognosis of HIV infections dramatically improved after introduction of highly active anti-retro viral therapy (HAART). However, the occurrence of adverse events and drug resistance during long-term use of anti-retrovirals are now big issues (Yeni et al., 2002; Dieleman et al., 2002). Present HAART also has a problem to maintain a high adherence because of the pill burden and patients' quality of life is affected. Combivir® is a fixed dose combination tablet containing zidovudine (ZDV) and lamivudine (3TC) (Eron et al., 2000). Each tablet contains 300 mg of ZDV and 150 mg of 3TC and has been widely used as a nucleoside reverse transcriptase inhibitor (NRTI) component of HAART against HIV-1 infection.

HIV infection and AIDS are known to be associated with a significant hematological toxicity, including anemia, neutropenia, and thrombocytopenia (Moses et al., 1998). In addition, studies with zidovudine have shown that this drug may compound the hematological toxicity of HIV and lead to an independent development of anemia and neutropenia (Wilde and Langtry, 1993). Consistent with these observations, the incidence of anemia or neutropenia in mildly or asymptomatic adults treated with zidovudine was between 1.1% and 9.7%, whereas in adults with AIDS or the AIDS related complex it ranged from 15% to as high as 61% (Wilde

* Corresponding author. Tel.: +81 96 373 6536; fax: +81 96 373 6537.
E-mail address: shuzo@kaiju.medic.kumamoto-u.ac.jp
(S. Matsushita).

1386-6532/$ – see front matter © 2004 Elsevier B.V. All rights reserved.
doi:10.1016/j.jcv.2004.11.002

and Langtry, 1993). In Japan, many physicians prescribe low dose ZDV such as 400 mg/day to avoid drug-induced anemia and neutropenia even though the standard dose of ZDV is 500–600 mg/day in United States (Kimura et al., 1992, 1998). Given the dose-dependent nature of these adverse effects, they are concerned about increased risk of hematological toxicity using Combivir that contains 600 mg of ZDV as the daily dose for Japanese patients who have lower body weights compared to patients in United States. Moreover, long-term consequence of the hematological toxicity resulting from continuous use of Combivir has not been well defined. We retrospectively reviewed clinical records of HIV-1 infected cases under treatment of Combivir-containing regimen used in three hospitals in Japan and we analyzed clinical data cross-sectionally to evaluate long-term toxicity of Combivir.

2. Patients and methods

HIV-1 positive Japanese patients were recruited from Kumamoto University Hospital, Osaka National Hospital and International Medical Center of Japan from June 1999 (after the Combivir launch) until June 2003. The clinical record was investigated in a retrospective manner. All collected cases were separated into four groups, as follows;

Primary Combivir Group (PCV): started Combivir as a first-line HAART.
Secondary Combivir Group (SCV): changed to Combivir from other NRTIs.
Primary Control Group (PCO): started NRTIs (except for Combivir) as a first-line HAART.
Secondary Control Group (SCO): changed to NRTIs except Combivir from other NRTIs.

We checked hemoglobin levels and neutrophil counts to examine the influence on hematological toxicity of ZDV every 6 months. We analyzed the data that could be followed over 18 months for removing various biases such as drop out cases with abnormal laboratory test values. Moreover, we also checked the HIV-RNA, $CD4^+$ T-cell counts and other laboratory test data every 6 months. We also checked any adverse events. This study was done under the approval of the Institutional Review Board of the Kumamoto University Hospital, Japan. All participants provided written informed consent.

3. Results

3.1. Patients' characteristics

Of the 94 data on subjects were 55 who were on Combivir (PCV: 27, SCV: 28) and 39 were on control regimens (PCO: 29, SCO: 10). The NRTIs used in the control group included of 20 cases of ZDV (400 mg/day) + 3TC, 18 cases of stavudine (d4T) + 3TC and one case of d4T + didanosine (ddI). Patients' characteristics are shown in Table 1. A couple of factors are statistically different such as the sex ($p < 0.01$: Fisher's exact test), weight ($p < 0.05$: Student's t-test) and Karnofsky score ($p = 0.0062$: Student's t-test) between Combivir group and control group. Combivir was likely to be used for patients with a higher baseline weight and the males. The mean viral load at baseline in Combivir group was $10^{3.9}$ copies/mL and for the control group was $10^{4.1}$ copies/mL. There was no statistical difference between the groups. The baseline $CD4^+$ T-cell counts in Combivir group were higher than in the control group significantly (393/mm^3 versus 263/mm^3; $p = 0.0101$: Student's t-test). Most patients were prescribed efavirenz (EFV) or nelfinavir (NFV) as a concomitant drug. Fifty-two percent of all patients were on EFV and 16% were taking NFV. The Combivir group had more combination cases with EFV than did the control group, because these two drugs approved for use in Japan at the same period have similar characteristics such as small pill counts and frequency of ingestion.

3.2. Effects on hemoglobin levels

To avoid biases in the data resulting from inclusion of patients with a shorter time follow up, including drop out cases, we focused on the patients that could be followed for over 18 months. Mean hemoglobin levels at baseline of Combivir group (PCV group: 13.9 g/dL, SCV group: 14.2 g/dL) were higher than for the control group (PCO group: 13.1 g/dL, SCO group: 13.7 g/dL) (Fig. 1A). It seems Combivir was likely to give to those with a lesser risk of anemia. We divided patients in PCV group into two sub-groups such as hemoglobin level decreased (sub-group A; $n = 10$) and not changed or increased (sub-group B: $n = 8$) at 6 months after starting Combivir. Fig. 1B shows a trend of hemoglobin levels in sub-group A. Each hemoglobin level at 6, 12, 18 and 24 months after starting treatment decreased significantly compared to baseline ($p < 0.005$, $p < 0.005$, $p < 0.005$ and $p < 0.05$, respectively; Wilcoxon matched pairs signed rank test). However, the decreased hemoglobin levels at 6 months gradually recovered to the baseline level despite continuation of the same regimen. The hemoglobin level at 18, 24 months increased significantly compared to 6-month values ($p < 0.05$ and $p < 0.005$, respectively). On the other hand, the hemoglobin level of sub-group B did not decrease for 18–30 months of follow up period (data not shown). The difference of background between sub-groups A and B was baseline level of hemoglobin and hematocrit. These levels in sub-group A were higher than for sub-group B statistically (14.9 ± 1.2 versus 12.6 ± 0.7; $p < 0.001$, 44.4 ± 3.2 versus 37.4 ± 2.0; $p < 0.001$, Student's t-test).

3.3. Effects on neutrophil counts

The trend of mean neutrophil counts was similar to counts for hemoglobin levels. Mean neutrophil counts of all groups

Table 1
Baseline characteristics

	Combivir group (PCV + SCV) ($n = 55$)	Control group (PCO + SCO) ($n = 39$)	p-value
Sex (male/female)	54/1	32/7	0.00815[a]
Age	35.9 ± 9.5 (22–68)	38.6 ± 10.7 (23–78)	0.2117[b]
Weight (kg)	64.6 ± 10.8 (47.0–91.6)	59.6 ± 11.2 (36.4–81.0)	0.0303[b]
Hemophilia			
Non	48	32	0.562[a]
A	5	7	
B	2	0	
Baseline VL (log)			
<2.6	19	11	0.4432[b]
2.6–3	1	1	
3–4	6	4	
4–5	11	13	
>5	15	10	
Unknown	3	0	
Mean ± S.D.	3.9 ± 1.2	4.1 ± 1.2	
Range	2.6–5.9	2.6–5.9	
Baseline CD4 count			
<200	14	14	0.0101[b]
200–500	25	19	
>500	13	5	
Unknown	3	1	
Mean ± S.D.	393 ± 265	263 ± 179	
Range	1–1132	5–607	
CDC class			
A1	5	3	0.8064[c]
A2	22	17	
A3	6	13	
B1	2	0	
B2	3	0	
B3	2	5	
C1	3	0	
C3	12	11	
Karnofsky score			
20%	0	1	0.0062[b]
40%	0	2	
50%	0	1	
60%	1	0	
70%	0	1	
80%	4	6	
90%	11	8	
100%	39	20	
Mean ± S.D.	95.8 ± 7.9	87.7 ± 19.4	

[a] Fisher' exact test.
[b] Student's t-test.
[c] Wilcoxon 2-sample test.

were over 2000/mm^3 and did not have statistically change from the baseline during the follow up period (Fig. 1C). We separated subjects in the PCV group into two sub-groups as well as for hemoglobin levels to examine the toxicity of Combivir to neutrophils. In the sub-group C ($n = 10$) those with mean neutrophil counts decreased and the sub-group D ($n = 7$) included subjects with no changes or increased neutrophil counts at 6 months after being on Combivir. Fig. 1D shows the trend of the neutrophil counts in sub-group C. Neutrophil counts at 6, 12, 18 and 24 months after starting the treatment decreased significantly compared to baseline ($p < 0.005$, $p < 0.05$, $p < 0.05$ and $p < 0.05$, respectively; Wilcoxon matched pairs signed rank test). However, the decreased neutrophil counts gradually recovered as did hemoglobin levels. The mean neutrophil counts at 18 months increased significantly compared to data at 6 months ($p < 0.05$; Wilcoxon matched pairs signed rank test).

3.4. Effects on other laboratory test value

MCV values at baseline for the secondary treatment group such as SCV group and SCO group were higher than for pri-

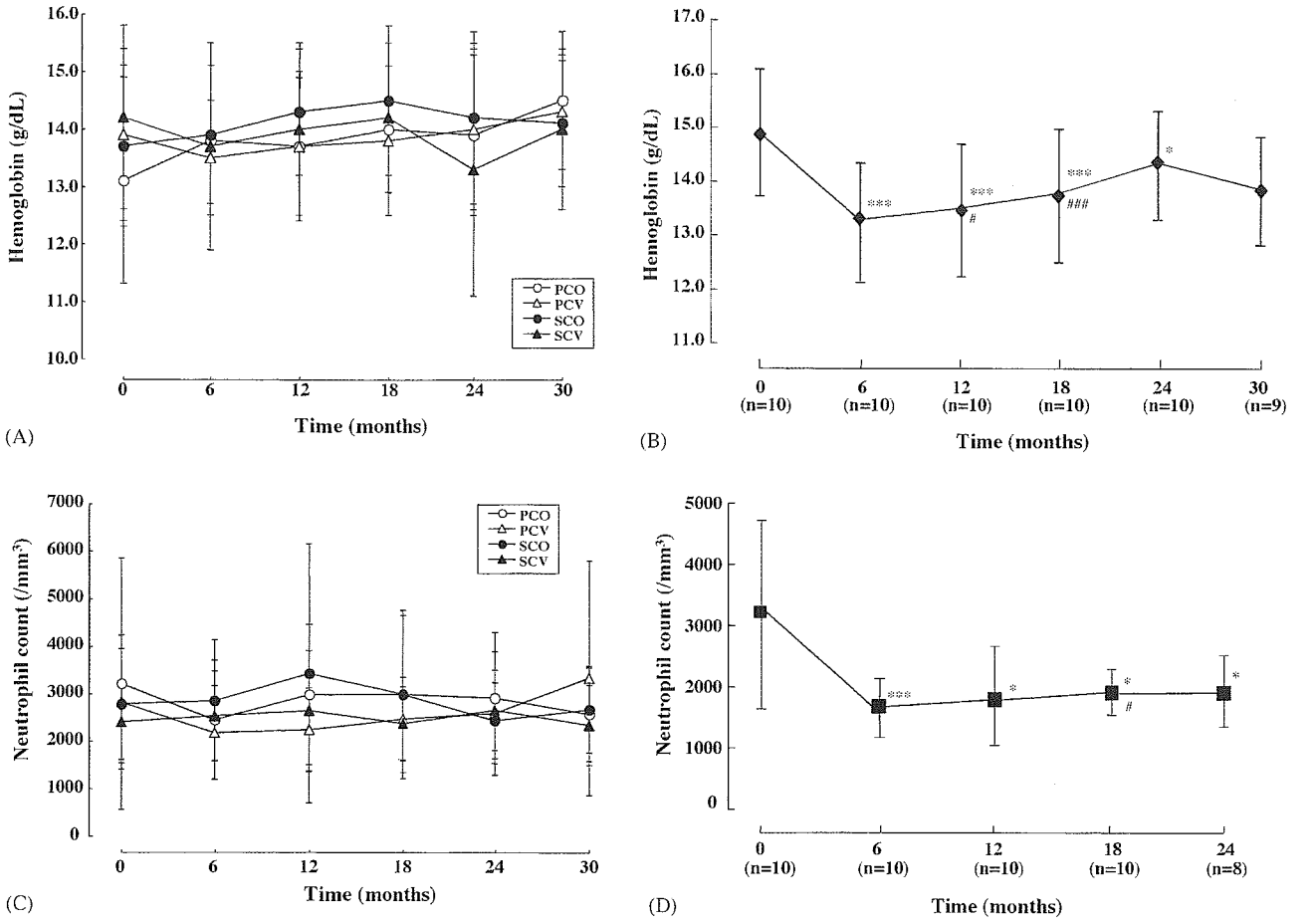

Fig. 1. Recovery after transient suppression of hemoglobin and neutrophil levels in patients with long-term use of Combivir. (A) Mean hemoglobin levels did not change significantly in all groups during each treatment. The baseline hemoglobin level in the Combivir group (PCV + SCV) was higher than in controls (PCO + SCO). (B) Mean hemoglobin levels at 6, 12, 18 and 24 months after start of treatment decreased significantly compared to baseline in the subgroup A of PCV group ($n = 10$). However the decreased hemoglobin level gradually reverted to the baseline levels despite continuation of the same regimen. Hemoglobin levels at 12 and 18 months were significantly high compared to findings at 6 months. (Wilcoxon matched pairs signed rank test; $^{*,\#}p < 0.05$, $^{***,\#\#\#}p < 0.005$). (C) Mean neutrophil counts did not change significantly in all groups during each treatment. (D) Mean neutrophil counts at 6, 12, 18 and 24 months after beginning treatment decreased significantly compared to baseline in sub-group C of PCV group ($n = 10$). However, the neutrophil counts gradually reverted to baseline levels despite continuation of the same regimen. The neutrophil counts at 18 months was significantly high compared to that of 6 months (Wilcoxon matched pairs signed rank test; $^{*,\#}p < 0.05$, $^{***}p < 0.005$).

mary treatment groups such as PCV group and PCO group. It seems ZDV or d4T in the secondary treatment group affected red blood cell counts. However, after starting each treatment, MCV values increased and became high at around 110/mm^3 in all groups (Fig. 2A). Other laboratory test values did showed no notable changes (data not shown).

3.5. Adverse events

The most common adverse events in each group were nausea/vomiting, dizziness and malaise. Anemia was observed in two in the Combivir group and one in the control group. Discontinuing each treatment led to elimination of these adverse effects. The anemia in two in the Combivir group was observed 2 months after their starting treatment, and that in one in the control group was evident as early as the eighth day. The occurrence of anemia in the control group was on ZDV 400 mg/day + 3TC. The frequency of anemia in the Combivir group was 3.6% (2/55) and similar to that in the control group {2.6% (1/39)}. The 20 in the control group on ZDV + 3TC regimen were on a ZDV 400 mg/day. We compared the safety profile of ZDV 600 mg/day to ZDV 400 mg/day. Adverse events rate of Combivir was 50.9% (28/55) and 60.0% (12/20) of AZT + 3TC group. Moreover, the number who discontinued Combivir group was 7 (12.7%) and that in ZDV + 3TC group was 5 (25.0%). In the SCV group, nineteen were changed to Combivir from ZDV 400 mg/day + 3TC. There were six with some adverse events and these were similar to other groups' events. These observations suggest that increasing the ZDV dose to 600 mg/day does not affect the incidence of adverse events. In addition there were no concomitantly used drugs that could affect pharmacokinetic parameters of ZDV and enhance its toxicity.

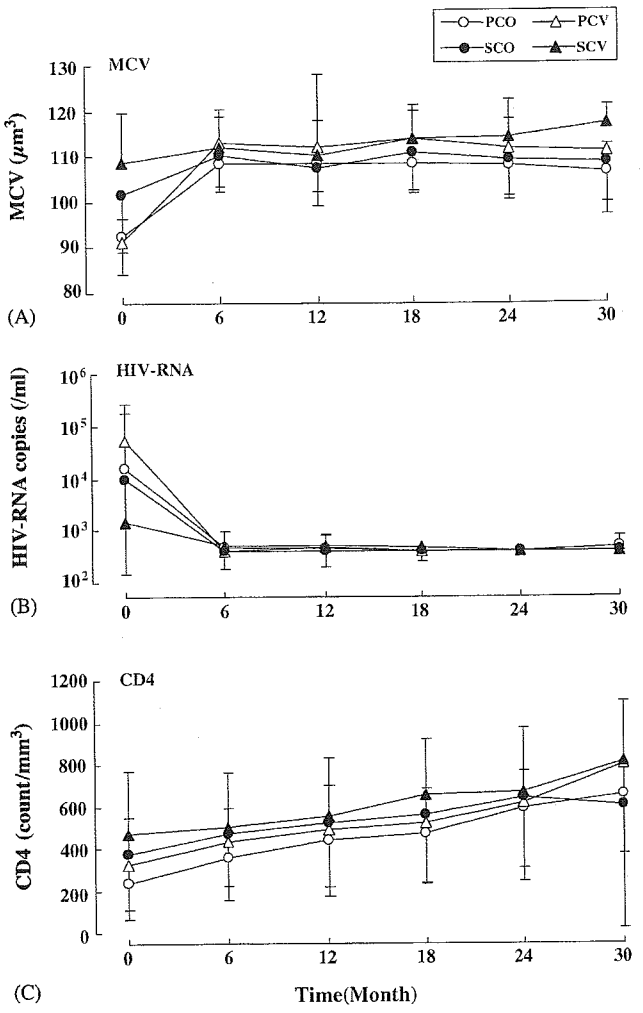

Fig. 2. Changes in MCV values, HIV RNA level and CD4+ T cell counts in each group of patients. (A) MCV values for the secondary treatment group such as SCV and SCO group were higher than for primary treatment groups such as PCV and PCO group at baseline. However, after starting each treatment, MCV values increased and became high at around 110/mm^3 in all groups. (B) Mean HIV RNA level in all groups of treatment decreased compared to baseline significantly ($p<0.05$–$p<0.001$; Wilcoxon matched pairs signed rank test). (C) Mean CD4+ T cell counts in all groups of treatment increased significantly compared to the baseline ($p<0.05$–$p<0.001$; Wilcoxon matched pairs signed rank test).

3.6. Effects on viral load and CD4+ T-cell counts

Baseline viral load in the primary treatment group (PCV + PCO) was higher than in the secondary treatment group (SCV + SCO). Mean baseline viral loads of each group were $10^{4.6}$ copies/mL (PCV), $10^{4.0}$ copies/mL (PCO), $10^{3.0}$ copies/mL (SCV) and $10^{3.7}$ copies/mL (SCO), respectively. However, after starting each treatment, HIV RNA was not detectable in serum samples from in each group (VL < 50 or <400 copies/mL) (Fig. 2B). Baseline CD4+ T-cell count in the SCV group was 518/mm^3 and higher than other groups (PCV: 304/mm^3, SCO: 345/mm^3, PCO: 277/mm^3) significantly ($p<0.001$; Student's t-test) (Fig. 2C). This result suggests effective treatment with the previous combination for the SCV group. CD4+ T-cell counts during each treatment increased significantly ($p<0.05$–$p<0.001$; Wilcoxon matched pairs signed rank test) and reached over 600/mm^3 at 30 months in all groups (Fig. 2C).

4. Discussion

The nucleoside reverse transcriptase inhibitor (NRTI) was first developed as an anti-HIV drug. However, the appropriate dosage was unclear because this type of drug is only active after being phosphorylated inside cells. A daily dose of 400 mg of ZDV has been widely used in Japan because anemia and neutropenia occurred frequently in cases of ingesting a higher dose (800 mg/day) than did 400 mg/day of ZDV in a clinical trial conducted in Japan (Kimura et al., 1992). Bone marrow toxicity associated with AZT such as macrocytic anemia and neutropenia has been frequently reported for the patients treated with a higher dose of ZDV mono therapy (Richman et al., 1987). Given the dose-dependent nature of these adverse effects, Japanese health care providers have some hesitance to prescribe Combivir that contains 600 mg of ZDV, as the daily dose. Data on four patients with severe anemia associated with Combivir have also been reported (Sibery et al., 2003). To evaluate the long-term toxicity of Combivir, we reviewed clinical records of HIV-1 infected Japanese patients on treatment with Combivir-containing regimen.

The results in this retrospective study showed that anemia and adverse events occurred at comparable frequency in each group of patients. Consistent with previous reports (Hester and Peacock, 1998; Tseng et al., 1998) these adverse events occurred in less than a few months after starting each treatment. The frequency of anemia in the Combivir group was only 3.7% (2/54), and it was similar to that for ZDV 400 mg/day + 3TC group (5.0%) group. In other words there was no difference in these groups with respect to the frequency of anemia by the difference in the dose of ZDV. It is also of note that the efficacy of Combivir was comparable to that of 400 mg of ZDV of four times a day with a twice a day dosing of 3TC. However, we have to take into account the fact that Combivir was prescribed for heavy weight patients. And such may mask the occurrence of adverse events as well as the difference in efficacy.

We observed a certain degree of decrease in hemoglobin levels and neutrophil counts in the subgroups of patients in PCV (subgroups A and C, respectively). Interestingly, a gradual recovery of these hematological toxicities occurred despite the continuation of Combivir containing regimens. The mechanism whereby the risk of hematological toxicity associated with increasing ZDV dosages may be related to the intracellular accumulation of the toxic metabolite zidovudine monophosphate (AZTMP) (Tornevik et al., 1995). AZTMP interferes with both cellular DNA synthesis and exonuclease-catalyzed removal of ZDV from host cell DNA (Sommadossi et al., 1989; Harrington et al., 1993). In addition, at clinically

relevant concentrations, AZTMP acts as a potent inhibitor of the transport of pyrimidine nucleotide sugars into the Golgi complex, thereby inhibiting protein glycosylation and altering glycosphingolipid synthesis (Yan et al., 1995). Therefore, AZTMP may elicit cytotoxic effects on rapidly growing erythrocytes and neutrophil precursors, both by interfering with nuclear DNA replication and by compromising the function of membrane receptors involved in receiving of extracellular stimuli required for cell growth and differentiation. From these observations it seems reasonable to speculate that either decrease in the intracellular concentration of AZTMP or compensatory mechanisms that improve the signal transduction for erythropoiesis and myelopoiesis mediated by cytokines contributed the recovery from hematological toxicities.

Two mechanisms may be related to the decrease in the concentration of AZTMP: altered metabolism of nucleoside analogues due to impaired nucleoside phosphorylation and increased efflux of the compounds by membrane transport mechanisms (Schuetz et al., 1999; Wijnholds et al., 2000). These mechanisms have been considered to contribute to the cellular drug-resistance (Dianzani et al., 1994; Groschel et al., 1997; Fridland et al., 2000; Turriziani et al., 2000). However, there was no evidence of treatment failure for patients in our PCV group as we found an increase in $CD4^+$ cell counts and an undetectable HIV-RNA load. Furthermore, the MCV level which is associated with the intracellular increase of AZTMP was kept high. These observations suggest that decrease in the level of AZTMP in the course of long-term treatment is unlikely although we must determine longitudinal changes of intracellular AZTMP level in precursors of blood cells in patients on Combivir treatment. Other compensatory mechanisms against the hematological toxicity may occur. An increase in erythropoietin or granulocyte-colony stimulating factor (G-CSF) levels in compensation for chronic anemia or neutropenia is another notion.

Acknowledgments

This work was supported in part by the Ministry of Health, Labor and Welfare of Japan (H-15-AIDS-001, -011, -015 and H-13-AIDS-001).

References

Dianzani F, Antonelli G, Turriziani O, Riva E, Simeoni E, Signoretti C, et al. Zidovudine induces the expression of cellular resistance affecting its antiviral activities. AIDS Res Hum Retroviruses 1994;10:1471–8.

Dieleman JP, Jambroes M, Gyssens IC, Sturkenboom MC, Stricker BH, Mulder WM, et al. Determinants of recurrent toxicity-driven switches of highly active antiretroviral therapy. The ATHENA Cohort. AIDS 2002;16:737–45.

Eron JJ, Yetzer ES, Ruane PJ, Becker S, Sawyerr GA, Fisher RL, et al. Efficacy, safety, and adherence with a twice-daily combination of lamivudine/zidovudine tablet formulation, plus a protease inhibitor, in HIV infection. AIDS 2000;14:671–81.

Fridland A, Connelly MC, Robbins BL. Cellular factors for resistance against antiretroviral agents. Antiviral Ther 2000;5:181–5.

Groschel B, Cinatl J, Cinatl Jr J. Viral and cellular factors for resistance against antiretroviral agents. Intervirology 1997;14:400–7.

Harrington JA, Reardon JE, Spector T. 3′-Azido-3′-deoxythymidine (AZT) monophosphate: an inhibitor of exonucleolytic repair of AZT terminated DNA. Antimicrob Agents Chemother 1993;37:918–20.

Hester EK, Peacock Jr JE. Profound and unanticipated anemia with lamivudine-zidovudine combination therapy in zidovudine-experienced patients with HIV infection. AIDS 1998;12:439–40.

Kimura S, Oka S, Toyoshima T, Hirabayashi Y, Kikuchi Y, Mitamura K, et al. A randomized trial of reduced doses of azidothymidine in Japanese patients with human immunodefiency virus type 1 infection. Intern Med 1992;31:871–6.

Kimura S, Yamada K, Ito A, Mimaya J, Takamatsu J, 3TC Study Group. Phase 2 clinical study on 3TC (Lamivudine) in HIV infections. Antibiot Chemother 1998;14:1419–32.

Moses A, Nelson J, Bagby Jr GC. Review article: the influence of human immunodeficiency virus-1 on hematopoiesis. Blood 1998;91:1479–95.

Richman DD, Fischl MA, Grieco MH, Gottlieb MS, Volberding PA, Laskin OL, et al. The toxicity of azidothymidine (AZT) in the treatment of patients with AIDS and AIDS-related complex. A double-blind, placebo-controlled trial. N Engl J Med 1987;317:192–7.

Schuetz JD, Connelly MC, Sun D, Paibir SG, Flynn PM, Srinivas RV, et al. MRP4: a previously unidentified factor in resistance to nucleoside-based antiviral drugs. Nat Med 1999;5:1048–51.

Sibery MJ, Astrow A, Kempin S, Halperin I. Combivir (AZT/3TC) therapy is associated with life-threatening anemia in patients with HIV infection. Blood 2003;102:51b (Abstract 3907).

Sommadossi JP, Carlisle R, Zhou Z. Cellular pharmacology of 3-azido-3′-deoxythymidine with evidence of incorporation into DNA of human bone marrow cells. Mol Pharmacol 1989;36:9–14.

Tornevik Y, Ullman B, Balzarini J, Wahren B, Eriksson S. Cytotoxicity of 3′-azido-3′-deoxythymidine correlates with 3′-azidothymidine-5′-monophosphate (AZTMP) levels, whereas anti-human immunodeficiency virus (HIV) activity correlates with 3′-azidothymidine-5′-triphosphate (AZTTP) levels in cultured CEM T-lymphoblastoid cells. Biochem Pharmacol 1995;49:829–37.

Tseng A, Conly J, Fletcher D, Keystone D, Salit I, Walmsley S. Precipitous declines in hemoglobin levels associated with combination zidovudine and lamivudine therapy. Clin Infect Dis 1998;27:908–9.

Turriziani O, Antonelli G, Dianzani F. Cellular factors involved in the induction of resistance of HIV to antiretroviral agents. Int J Antimicrob Agents 2000;16:353–6.

Wijnholds J, Mol CA, van Deemter L, de Haas M, Scheper GL, Baas F, et al. Multidrug-resistance protein 5 is a multispecific organic anion transporter able to transport nucleotide analogs. Proc Natl Acad Sci USA 2000;97:7476–81.

Wilde MI, Langtry HD. Zidovudine. An update of its pharmacodynamic and pharmacokinetic properties, and therapeutic efficacy. Drugs 1993;46:515–78.

Yan JP, Ilsley DD, Frohlick C, et al. 3′-Azidothymidin (zidovudine) inhibits glycosylation and dramatically alters glycosphingolipid synthesis in whole cells at clinically relevant concentrations. J Biol Chem 1995;270:22836–41.

Yeni PG, Hammer SM, Carpenter CCJ, Cooper DA, Fischl MA, Gatell JM, et al. Antiretroviral treatment for adult HIV infection. 2002. Updated recommendation of the International AIDS Society-USA Panel. JAMA 2002;288:222–35.

Generation of High-Affinity Antibody against T Cell-Dependent Antigen in the *Ganp* Gene-Transgenic Mouse[1]

Nobuo Sakaguchi,[2]*¶ Tetsuya Kimura,† Shuzo Matsushita,† Satoru Fujimura,* Junji Shibata,† Masatake Araki,‡ Tamami Sakamoto,§ Chiemi Minoda,§ and Kazuhiko Kuwahara*‖

Generation of high-affinity Ab is impaired in mice lacking germinal center-associated DNA primase (GANP) in B cells. In this study, we examined the effect of its overexpression in *ganp* transgenic C57BL/6 mice (*Ganp*^{Tg}). *Ganp*^{Tg} displayed normal phenotype in B cell development, serum Ig levels, and responses against T cell-independent Ag; however, it generated the Ab with much higher affinity against nitrophenyl-chicken gammaglobulin in comparison with C57BL/6. To further examine the affinity increase, we established hybridomas producing high-affinity mAbs and compared their affinities using BIAcore. C57BL/6 generated high-affinity anti-nitrophenyl mAbs ($K_D \sim 2.50 \times 10^{-7}$ M) of IgG1/λ1 and contained the V_H*186.2* region with W33L mutation. *Ganp*^{Tg} generated much higher affinity ($K_D > 1.57 \times 10^{-9}$ M) by usage of V_H*186.2* as well as noncanonical V_H*7183* regions. *Ganp*^{Tg} also generated exceptionally high-affinity anti-HIV-1 (V3 peptide) mAbs ($K_D > 9.90 \times 10^{-11}$ M) with neutralizing activity. These results demonstrated that GANP is involved in *V* region alteration generating high-affinity Ab. *The Journal of Immunology,* 2005, 174: 4485–4494.

The Ag-driven B cells expressing high-affinity BCR, which have been selected in secondary lymphoid organs, generate high-affinity Ab. Ag-driven B cells proliferate rapidly by the stimulation with Ag and costimulatory molecules from Th cells surrounding the germinal center (GC)[3] region, in which such B cells undergo affinity maturation of Ig V region and class switching of the C region during the response to T cell-dependent Ag (TD-Ag) in vivo (1, 2). For affinity maturation, introduction of somatic hypermutation (SHM) in the *V* region is probably essential and, in addition to this molecular alteration, the Ag-driven B cells with high-affinity BCR must be selected or further enriched during the maturation of Ag-driven B cells in GCs.

A 210-kDa germinal center-associated DNA primase (GANP) protein, bearing RNA-primase and minichromosome maintenance (MCM)3-binding activities, is up-regulated in GC B cells upon immunization with TD-Ag in vivo and is induced by the stimulation to BCR and CD40 in vitro (3, 4). The mutant mouse with *ganp* gene knockout B cells (B-*ganp*$^{-/-}$) has a severe defect in mounting high-affinity Ab responses to TD-Ag (5), suggesting that GANP is required for generation of high-affinity Ab in response to TD-Ag in vivo. However, there remained several possibilities to account for the molecular mechanism in generation of high-affinity V regions by the expression of GANP in GC B cells. GANP might augment the induction of SHM in the *V* regions, resulting in the affinity maturation of V regions during the proliferation and differentiation of Ag-driven B cells in GCs. Alternatively, GANP might be involved in the survival of the high-affinity BCR$^+$ B cells for the positive selection through the interaction of Ags captured on the follicular dendritic cell network. The GCs of the B-*ganp*$^{-/-}$ mice displayed an increase of apoptotic cells upon immunization with TD-Ag SRBC, which suggested a partial involvement of GANP in the survival of GC B cells. However, the *ganp*$^{-/-}$ B cells do not show marked abnormalities in the levels of apoptotic and proapoptotic molecules after BCR cross-linkage (5). To study the function of GANP in generation of high-affinity Ab response, it is necessary to examine whether the affinity maturation of BCR on the GC B cell is generated by the genetic alteration in the *V* region gene.

We speculated that it would be possible to generate a high-affinity Ab if we used mice with higher level GANP expression in B cells. We studied whether the transgenic mouse with increased expression of *ganp* gene could generate high-affinity Ab against TD-Ag using a model epitope of 4-hydroxy-3-nitrophenyl acetyl (NP)-hapten in the C57BL/6 background. To demonstrate the increased affinity of the Ab in detail, we established the hybridomas secreting anti-NP mAbs after immunization with NP-chicken gammaglobulin (CG) in *Ganp*^{Tg} mice. After selecting the high-affinity mAbs against NP-hapten by differential ELISA method and the BIAcore system, we examined the *V* region gene usage of the hybridomas and compared the sequences with those from wild-type C57BL/6 mice. The results suggest that the affinity maturation of BCR on GC B cells is generated by the altered V_H region usage with increased SHM in *Ganp*^{Tg} mice.

Materials and Methods

Ganp^{Tg} *mouse*

The expression construct of mouse *ganp* cDNA under the mouse Ig promoter and human Ig enhancer (6) was used for establishing the transgenic

*Department of Immunology, Graduate School of Medical Sciences, †Division of Clinical Retrovirology and Infectious Diseases, Center for AIDS Research, ‡Division of Bioinformatics, Institute of Resource Development and Analysis, Kumamoto University, and §Trans Genic, Kumamoto Japan; ¶Core Research for Evolutional Science and Technology Program, Saitama Japan; and ‖PRESTO, Japan Science and Technology Agency, Saitama, Japan

Received for publication October 26, 2004. Accepted for publication January 4, 2005.

The costs of publication of this article were defrayed in part by the payment of page charges. This article must therefore be hereby marked *advertisement* in accordance with 18 U.S.C. Section 1734 solely to indicate this fact.

[1] This work was supported by Special Coordination Funds for Promoting Science and Technology from the Ministry of Education, Culture, Sports, Science and Technology of Japan, Matching Funds from New Energy and Industrial Technology Development Organization, and grants from the Core Research for Evolutional Science and Technology Program, Japan Science and Technology Agency.

[2] Address correspondence and reprint requests to Dr. Nobuo Sakaguchi, Department of Immunology, Graduate School of Medical Sciences, Kumamoto University, 1-1-1, Honjo, Kumamoto 860-8556, Japan. E-mail address: nobusaka@kaiju.medic.kumamoto-u.ac.jp

[3] Abbreviations used in this paper: GC, germinal center; GANP, germinal center-associated DNA primase; NP, 4-hydroxy-3-nitrophenyl acetyl; SHM, somatic hypermutation; TD-Ag, T cell-dependent Ag; MCM, minichromosome maintenance; CG, chicken gammaglobulin; KLH, keyhole limpet hemocyanin; TNP, 2,4,6-trinitrophenyl; LTR, long terminal repeat.

0022-1767/05/$02.00